18. MAJOR ELEMENT COMPOSITION OF LEG 92 SEDIMENTS[1]

Mitchell W. Lyle, College of Oceanography, Oregon State University[2]

ABSTRACT

The major element composition of Leg 92 sediments reflects the input of hydrothermal precipitates from the East Pacific Rise and extinct Mendoza Rise plus minor amounts of terrigenous detritus. The basal sediments are a mixture of hydrothermally precipitated ferromanganese oxyhydroxides and carbonates. In present and ancient sediments deposited 200 km or more from the rise crest, however, the amount of hydrothermal precipitates in the sediments decreases markedly. The distal deposits of hydrothermal particulates are also richer in iron because of fractionation by sedimentation processes. Slowly accumulating aluminosilicate detritus becomes a more important fraction of the sediments far from the rise crest as a result of the decrease of hydrothermal sedimentation.

INTRODUCTION

One of the goals of the Leg 92 drilling was to study the past and present geographic distribution of hydrothermally derived sediments from the East Pacific Rise (EPR). The drilling transect was located at 19°S for a variety of reasons; among other things, the region is in a flow line from the fastest-spreading segment of the mid-ocean ridge system, and the region lies underneath a hydrothermal plume emanating from the EPR (Lupton and Craig, 1981; Reid, 1982). The region lacks large inputs of organic matter to the sediments, and thus postdepositional modification of the sediments during early diagenesis is at a minimum. For example, Gieskes et al. (this volume) show evidence only for dissolution of calcite in the upper portions of Sites 597 and 598, and possibly 599, and no evidence for formation of new diagenetic minerals. There is no evidence that redox processes have ever modified the composition of the sediments significantly. The present-day distribution of nitrate and ammonia in the pore waters at all the sites in the Leg 92 transect (Gieskes et al., this volume) indicates that the typical pE of the sediments is too oxic for even the reduction and remobilization of manganese, the most redox-sensitive of the common transition metals. There is also no evidence for any long-term changes in productivity (e.g., changes in carbonate accumulation; Leinen, this volume) that could cause less oxic sedimentary redox conditions in the past.

The input of continental detritus is also very low. Sources for detrital material to this region are at least 4000 km away (Dymond, 1981), and the data of Bloomstine and Rea (this volume) indicate that the eolian detrital component has accumulated 1 to 2 orders of magnitude more slowly than in similar regions in the North Pacific. It is therefore an ideal place to study the composition of precipitates from a hydrothermal plume and to determine whether the composition of the plume-derived material was different during hydrothermal activity in the past.

This particular chapter is limited to an examination of the composition of the plume-derived precipitates (as well as other sediment components) and the depositional processes that could change the composition of the plume-derived material.

LOCATION AND SEDIMENTATION AT THE DRILL SITES

Figure 1 shows the locations of the three sites, 597, 598, and 599, that were sampled for this study. Hole 597 lies farthest west and was drilled into the oldest basement (28.6 Ma). The crust was actually formed at the extinct Mendoza Rise, but the rates of crustal formation are similar to those found today at the EPR. Hole 598 is located on the EPR proper, on 16.0-Ma crust, and Hole 599 is located on 7.8-Ma crust. There are 52.7 m of sediment at Hole 597, 52.4 m at Hole 598, and 40.8 m at Site 599, as summarized in the sedimentation rate curves for the three sites (Fig. 2). In the basal section of each hole, sedimentation rates range from 5 to 15 m/m.y., but upcore the rates decrease to 0.5 m/m.y. or less. The decline in sedimentation rate is due primarily to the increasing depth of each site and the increased dissolution of calcite (Rea and Leinen, this volume). The site survey for 597 and a limited survey for 598 show the area around each site to have low relief and a uniform sediment cover. There is little likelihood that sediment redeposition has occurred at either site. Site 599, on the other hand, is located in a small valley at the base of a slope; the presence of turbidites indicates that some of the section is redeposited upslope sediment (see Site 599 chapter, this volume).

The sediments themselves are similar at all three sites. They are primarily mixtures of coccolith calcite, clay, and red brown to yellow brown semiopaque oxides (RSO). The RSO fraction is similar to that found during DSDP Leg 34 in the sediments of the Bauer Basin (Yeats, Hart, et al., 1976). The Leg 92 sediments contain no discernible opaline material in smear slides, and no siliceous microfossils could be sieved from core-catcher samples.

[1] Leinen, M., Rea, D. K., et al., *Init. Repts. DSDP*, 92: Washington (U.S. Govt. Printing Office).

[2] Address: College of Oceanography, Oregon State University, Corvallis, OR 97331.

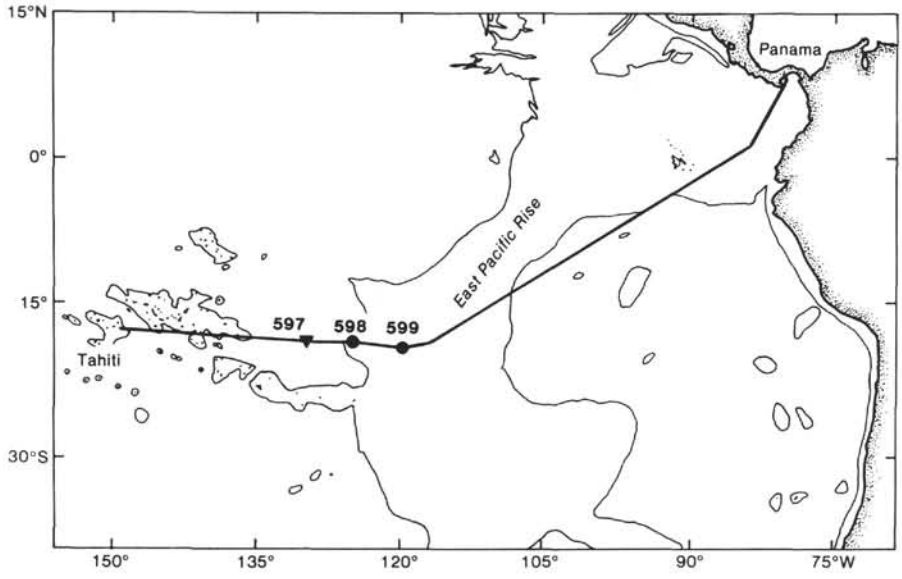

Figure 1. Location of Sites 597, 598, and 599 with respect to the major features of the southeast Pacific Ocean. Inverted triangle denotes re-entry.

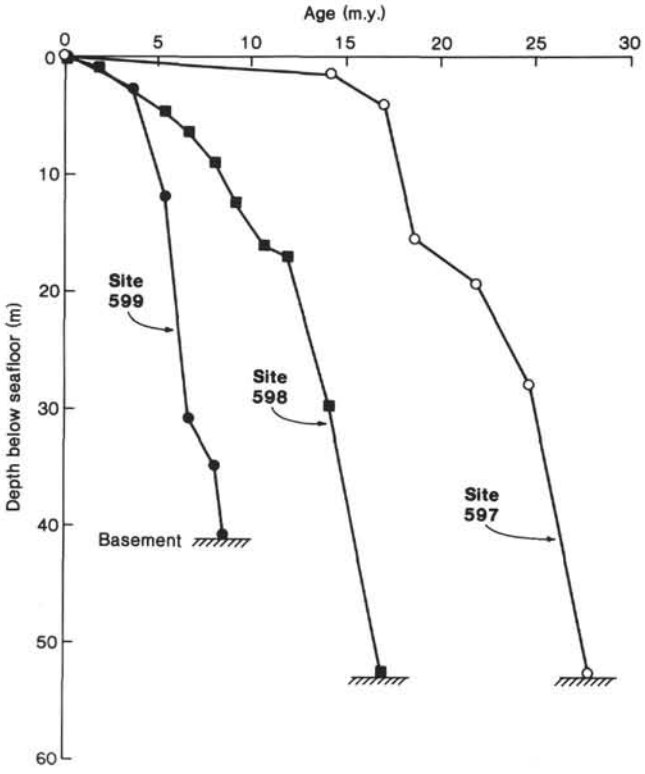

Figure 2. Sedimentation rate curves for Sites 597, 598, and 599 based upon Knüttel (this volume) and Romine (this volume). All three sites have the fastest sedimentation rates (≈ 10 mm/1000 yr.) when near the EPR crest; the sedimentation rates slow as the sites drop through the lysocline and calcite compensation depth.

Foraminifers are present but generally compose less than 5% of the total sediment.

SAMPLING AND ANALYTICAL METHODS

I studied Hole 598 in the greatest detail because it had the most complete, least complicated sedimentary record of the three sites. An entire 9.5-m section was lost during the coring of Hole 597 because of a core-catcher failure, so about 20% of the total sedimentary section was missing at the time of sampling. Subsequent efforts have correlated Holes 597 and 597A, so it will be possible to study this site in more detail in the future. The sedimentary record of Hole 599 is complicated by the local redeposition of sediments from the surrounding terrain. Several turbidites were found during core description, and reworked microfossils are abundant in a 25-m section of the core. In order to obtain a general record of the sedimentation at Holes 597 and 599, I analyzed a small set of samples (taken at intervals of approximately 1 m) from each of these holes. Hole 598, in contrast, was sampled at approximately 10-cm intervals for the entire length of the hole.

All sediment samples were freeze dried, ground in an agate mortar to disaggregate them, and pressed into pellets for X-ray fluorescence analysis. They were then analyzed on a Phillips PW1600 X-ray fluorescence spectrometer for Na, Mg, Al, Si, P, K, Ca, Ti, Mn, Fe, Ba, S, and Cl. Machine drift and power fluctuations were corrected for by analyzing a monitor standard (Canadian CCRMP standard syenite, SY-3) between each sample analysis. Raw counts were converted to elemental concentrations through the use of a fundamental parameters program and by further linear corrections derived from calibration with pressed pellets of over 100 N.B.S., U.S.G.S., Canadian, French, British, and South African standard geological materials, including sets of N.B.S. standards mixed with reagent-grade $CaCO_3$ to approximate calcite-rich sediments. The sedimentary compositions were then corrected for mass dilution by sea salt by assuming that all chlorine in the samples was derived from sea salt and by normalizing compositions to a salt-free mass. Further corrections for sea-salt additions in Na, Mg, K, Ca, and S were made by assuming that salt contains the same elemental ratios to chlorine as are found in average seawater and subtracting the salt component of these elements from the uncorrected concentrations. Calcium carbonate was also estimated by using the normative approach given in Dymond et al. (1976), which is based upon Ca abundance. The compositional information is presented in Table 1.

I checked the precision of our analyses by analyzing an in-house sediment standard with each sample set. For 330 analyses bracketing the time when the Leg 92 samples were run, the precision (1σ) was 8.0% for Na, 3.1% for Mg, 3.6% for Al, 3.3% for Si, 3.5% for P, 9.3% for Cl, 2.7% for K, 2.6% for Ca, 2.3% for Ti, 2.7% for Mn, 2.3% for Fe, 2.7% for Ba, and 16.1% for S. I was also able to check the accuracy of our Al, Si, Ca, Mn, Fe, and Ba analyses for a high-carbonate, transition metal-rich matrix typical of EPR sediments by comparing the results of analyzing 12 EPR sediments by our X-ray fluorescence (XRF) procedure with the results of Dymond's (1981) analysis by atomic absorption (AA) spectrophotometry. There is no signif-

Table 1. Bulk elemental composition of Site 597, 598, and 599 sediments (wt.%).

Core-Section (level in cm)	Sub-bottom depth (m)	Na	Mg	Al	Si	P	K	Ca	Ti	Mn	Fe	Ba	S
Site 597													
1-1, 13	0.13	1.137	1.442	4.001	11.67	0.932	1.411	10.5	0.340	2.99	10.61	0.215	0.121
1-1, 53	0.53	1.864	1.846	4.317	13.05	1.278	1.586	3.4	0.268	3.52	14.40	0.172	0.100
1-1, 101	1.01	1.896	1.982	3.303	9.46	1.079	0.986	2.8	0.190	3.49	18.24	0.177	0.090
1-2, 13	1.63	0.157	0.704	0.614	1.73	0.197	0.136	28.8	0.052	1.31	9.27	0.072	0.042
1-2, 72	2.23	0.130	0.619	0.499	1.42	0.120	0.121	30.7	0.047	1.13	7.49	0.074	0.038
1-3, 13	3.13	0.139	0.680	0.541	1.56	0.135	0.114	29.3	0.046	1.40	9.89	0.078	0.043
1-3, 93	3.93	0.357	0.593	0.463	1.42	0.125	0.104	28.6	0.046	1.49	9.77	0.082	0.030
2-1, 23	4.83	0.122	0.631	0.481	1.40	0.122	0.105	30.0	0.044	1.31	9.08	0.075	0.038
2-1, 73	5.53	0.162	0.642	0.473	1.43	0.127	0.095	29.7	0.047	1.41	9.50	0.079	0.039
2-1, 133	5.93	0.117	0.481	0.288	0.93	0.074	0.063	32.7	0.034	1.02	6.24	0.071	0.032
2-2, 73	6.83	0.301	0.910	0.605	1.95	0.174	0.114	24.2	0.050	2.52	13.97	0.085	0.049
2-2, 133	7.43	0.185	0.504	0.243	0.91	0.074	0.054	32.1	0.035	1.32	6.85	0.072	0.029
2-3, 93	8.53	0.184	0.498	0.220	0.83	0.068	0.048	33.6	0.031	1.20	5.73	0.078	0.034
2-4, 123	10.33	0.162	0.423	0.172	0.67	0.049	0.043	34.6	0.027	0.88	4.30	0.062	0.031
2-5, 73	11.33	0.101	0.443	0.223	0.82	0.054	0.053	34.2	0.031	0.74	5.07	0.065	0.033
2-6, 143	13.53	0.080	0.304	0.174	0.61	0.030	0.058	37.2	0.031	0.30	1.99	0.057	0.025
2-7, 3	13.63	0.039	0.307	0.156	0.56	0.025	0.061	37.3	0.028	0.24	1.59	0.055	0.022
3-3, 3	17.23	0.106	0.399	0.235	0.80	0.039	0.067	34.8	0.033	0.59	3.46	0.058	0.025
3-3, 73	17.93	0.121	0.371	0.199	0.73	0.035	0.064	35.4	0.033	0.55	3.41	0.057	0.019
3-4, 103	19.73	0.165	0.399	0.211	0.76	0.044	0.060	35.5	0.032	0.64	3.41	0.056	0.029
3-5, 93	21.13	0.132	0.342	0.171	0.63	0.030	0.055	35.5	0.033	0.47	2.24	0.051	0.024
3-6, 63	22.33	0.084	0.413	0.177	0.71	0.038	0.061	35.6	0.031	0.75	3.25	0.060	0.031
4-1, 83	24.63	0.144	0.420	0.178	0.75	0.041	0.060	34.4	0.030	1.15	3.99	0.065	0.031
4-2, 73	26.03	0.164	0.452	0.212	0.89	0.053	0.073	33.8	0.035	1.49	4.81	0.066	0.029
4-3, 63	27.43	0.325	0.513	0.207	0.88	0.056	0.063	33.0	0.038	1.69	5.29	0.064	0.033
4-4, 73	29.03	0.209	0.548	0.243	1.01	0.063	0.077	32.7	0.038	1.84	6.38	0.070	0.030
4-5, 93	30.73	0.189	0.477	0.185	0.82	0.058	0.063	34.4	0.031	1.49	4.93	0.069	0.029
4-6, 53	31.83	0.190	0.513	0.227	0.94	0.056	0.068	33.2	0.034	1.55	5.74	0.071	0.032
6-1, 83	43.83	0.314	0.670	0.364	1.24	0.124	0.111	29.9	0.055	2.67	7.57	0.064	0.037
6-2, 73	45.23	1.335	0.841	0.405	1.39	0.182	0.099	26.8	0.053	3.70	10.11	0.073	0.026
6-3, 102	47.03	0.362	0.529	0.512	1.69	0.118	0.213	32.8	0.114	1.84	4.45	0.059	0.036
6-4, 70	48.20	1.137	0.814	0.628	2.02	0.132	0.217	28.4	0.128	2.90	8.85	0.073	0.022
6-5, 67	49.63	0.361	0.591	0.383	1.28	0.092	0.141	33.1	0.080	1.71	4.62	0.058	0.028
6-5, 129	50.30	0.442	0.853	0.350	1.16	0.150	0.095	29.9	0.054	2.77	8.30	0.068	0.032
6-6, 83	51.33	0.545	1.076	0.685	2.23	0.183	0.202	27.7	0.123	2.88	8.84	0.081	0.037
Site 598													
1-1, 9	0.09	0.243	0.444	0.393	1.16	0.081	0.082	35.0	0.056	0.63	2.14	0.129	0.074
1-1, 19	0.19	0.120	0.539	0.643	1.85	0.140	0.137	32.9	0.084	1.05	3.85	0.169	0.097
1-1, 29	0.29	0.112	0.564	0.668	1.93	0.146	0.157	32.8	0.087	1.09	4.05	0.174	0.097
1-1, 39	0.39	0.296	0.729	1.115	3.14	0.262	0.271	29.4	0.130	1.74	6.75	0.220	0.113
1-1, 49	0.49	0.330	0.917	1.460	4.09	0.350	0.345	25.6	0.158	2.11	8.39	0.254	0.141
1-1, 59	0.59	0.300	0.895	1.462	4.13	0.353	0.343	25.7	0.161	2.06	8.21	0.244	0.137
1-1, 69	0.69	0.739	1.106	2.117	5.76	0.508	0.475	21.9	0.197	2.47	10.23	0.291	0.136
1-1, 79	0.79	0.577	1.038	1.809	4.95	0.430	0.397	24.2	0.191	2.30	9.53	0.257	0.139
1-1, 89	0.89	0.696	0.911	1.565	4.25	0.367	0.339	25.3	0.165	2.00	8.72	0.190	0.101
1-1, 99	0.99	0.290	0.813	1.253	3.43	0.302	0.284	28.2	0.141	1.73	7.75	0.173	0.108
1-1, 109	1.09	0.185	0.682	0.981	2.72	0.240	0.227	30.3	0.115	1.42	6.42	0.159	0.092
1-1, 119	1.19	0.185	0.602	0.825	2.31	0.208	0.194	31.2	0.098	1.23	5.69	0.163	0.084
1-1, 129	1.29	0.249	0.533	0.638	1.78	0.148	0.151	33.0	0.071	0.91	4.10	0.150	0.042
1-1, 139	1.39	0.189	0.391	0.393	1.16	0.092	0.105	34.9	0.053	0.61	2.76	0.123	0.062
1-2, 9	1.59	0.142	0.516	0.610	1.70	0.161	0.153	33.0	0.074	0.95	4.80	0.125	0.076
1-2, 18	1.68	0.090	0.452	0.483	1.37	0.133	0.120	34.2	0.064	0.78	3.94	0.108	0.060
1-2, 30	1.80	0.130	0.534	0.639	1.76	0.175	0.162	32.8	0.078	1.00	5.13	0.103	0.065
1-2, 39	1.89	0.161	0.566	0.655	1.75	0.174	0.151	32.7	0.071	0.98	5.01	0.099	0.039
1-2, 49	1.99	0.142	0.601	0.740	1.99	0.212	0.171	32.4	0.083	1.17	6.30	0.108	0.075
1-2, 59	2.09	0.241	0.830	1.123	2.96	0.337	0.256	27.0	0.112	1.67	9.42	0.115	0.091
1-2, 69	2.19	0.427	1.192	1.754	4.52	0.542	0.384	20.4	0.153	2.35	13.22	0.135	0.118
1-2, 102	2.53	0.645	1.209	1.874	4.87	0.584	0.455	19.6	0.152	2.40	14.31	0.148	0.119
1-2, 109	2.59	0.738	1.057	1.873	4.81	0.552	0.421	20.2	0.138	2.19	13.36	0.146	0.112
1-2, 119	2.69	0.356	1.099	1.516	4.00	0.545	0.343	21.7	0.127	2.17	13.30	0.156	0.126
1-2, 129	2.79	0.330	0.927	1.153	3.02	0.390	0.257	26.0	0.100	1.76	10.59	0.139	0.060
1-2, 139	2.89	0.134	0.595	0.676	1.85	0.236	0.168	31.1	0.073	1.15	6.98	0.139	0.079
1-2, 149	2.99	0.081	0.447	0.440	1.25	0.153	0.119	33.6	0.052	0.81	4.83	0.131	0.064
1-3, 9	3.09	0.026	0.375	0.318	0.94	0.104	0.084	35.0	0.043	0.61	3.59	0.113	0.038
1-3, 19	3.19	−0.002	0.371	0.293	0.88	0.099	0.079	35.1	0.042	0.58	3.42	0.099	0.038
1-3, 29	3.29	0.100	0.437	0.350	1.01	0.113	0.090	34.8	0.045	0.65	3.76	0.102	0.032
1-3, 39	3.39	0.112	0.518	0.478	1.39	0.148	0.115	33.6	0.054	0.87	5.13	0.114	0.043
1-3, 49	3.49	0.213	0.728	0.786	2.11	0.254	0.176	30.0	0.072	1.30	7.78	0.128	0.051
1-3, 59	3.59	0.225	0.711	0.781	2.09	0.250	0.172	30.0	0.070	1.30	7.86	0.132	0.048
1-3, 69	3.69	0.145	0.720	0.805	2.18	0.276	0.182	29.2	0.076	1.38	8.68	0.139	0.082
1-3, 79	3.79	0.142	0.578	0.546	1.51	0.177	0.124	32.5	0.056	0.97	5.98	0.131	0.044
1-3, 89	3.89	0.126	0.484	0.396	1.19	0.125	0.096	34.6	0.046	0.73	4.58	0.124	0.044
1-3, 99	0.99	0.022	0.356	0.248	0.77	0.85	0.063	35.3	0.036	0.51	3.09	0.115	0.034

Table 1 (continued).

Core-Section (level in cm)	Sub-bottom depth (m)	Na	Mg	Al	Si	P	K	Ca	Ti	Mn	Fe	Ba	S
Site 598 (Cont.)													
1-3, 109	4.09	0.060	0.357	0.238	0.74	0.085	0.058	35.4	0.035	0.47	2.91	0.106	0.030
1-3, 119	4.19	0.106	0.408	0.309	0.92	0.116	0.071	34.6	0.041	0.61	3.88	0.114	0.054
1-3, 129	4.29	0.121	0.364	0.254	0.78	0.095	0.060	35.2	0.035	0.50	3.10	0.111	0.030
1-3, 139	4.39	0.009	0.360	0.198	0.63	0.070	0.050	36.2	0.031	0.40	3.30	0.107	0.031
1-4, 9	4.59	0.287	0.328	0.164	0.54	0.060	0.037	36.8	0.028	0.32	1.95	0.092	0.014
1-4, 19	4.69	0.018	0.409	0.261	0.78	0.089	0.057	35.0	0.035	0.52	3.35	0.102	0.034
1-4, 29	4.79	0.015	0.463	0.336	0.97	0.121	0.070	34.4	0.040	0.69	4.59	0.099	0.037
1-4, 39	4.89	0.148	0.661	0.604	1.66	0.258	0.118	30.0	0.057	1.25	8.68	0.111	0.074
1-4, 49	4.99	0.386	0.872	0.872	2.41	0.347	0.146	26.7	0.068	1.65	11.06	0.129	0.060
1-4, 59	5.09	0.162	0.671	0.568	1.55	0.222	0.104	30.8	0.052	1.15	7.73	0.120	0.045
1-4, 69	5.19	0.089	0.442	0.283	0.85	0.102	0.064	34.9	0.035	0.60	4.03	0.113	0.033
1-4, 89	5.39	0.000	0.319	0.163	0.57	0.054	0.045	36.3	0.027	0.36	2.27	0.105	0.030
1-4, 99	5.49	0.156	0.348	0.174	0.59	0.055	0.044	36.5	0.027	0.38	2.39	0.105	0.023
1-4, 109	5.59	0.012	0.327	0.157	0.55	0.050	0.043	36.5	0.027	0.34	2.18	0.106	0.029
1-4, 119	5.69	0.043	0.351	0.155	0.54	0.049	0.046	37.0	0.027	0.32	2.01	0.101	0.028
1-4, 129	5.79	0.148	0.404	0.244	0.78	0.078	0.064	35.8	0.032	0.51	3.39	0.121	0.029
1-4, 139	5.89	0.067	0.437	0.319	0.99	0.104	0.081	34.2	0.035	0.66	4.56	0.122	0.036
1-4, 149	5.99	0.213	0.454	0.349	1.07	0.106	0.089	34.2	0.035	0.66	4.55	0.137	0.029
2-1, 7	6.27	0.141	0.327	0.118	0.54	0.034	0.040	36.7	0.024	0.23	1.68	0.097	0.017
2-1, 19	6.39	−0.023	0.324	0.112	0.52	0.034	0.042	36.2	0.023	0.24	1.69	0.096	0.026
2-1, 39	6.59	0.153	0.358	0.125	0.58	0.036	0.043	37.4	0.024	0.24	1.74	0.098	0.026
2-1, 49	6.69	0.237	0.319	0.120	0.54	0.037	0.038	36.6	0.024	0.25	1.75	0.098	0.020
2-1, 69	6.89	0.158	0.326	0.122	0.54	0.035	0.040	37.0	0.024	0.24	1.74	0.097	0.016
2-1, 79	6.99	0.024	0.355	0.130	0.55	0.038	0.045	37.0	0.024	0.26	1.89	0.098	0.025
2-1, 89	7.09	0.030	0.341	0.127	0.56	0.037	0.043	37.0	0.024	0.24	1.79	0.097	0.025
2-1, 99	7.19	0.061	0.360	0.126	0.56	0.036	0.046	37.5	0.024	0.25	1.82	0.098	0.026
2-1, 109	7.29	0.110	0.345	0.129	0.56	0.036	0.042	37.1	0.024	0.25	1.84	0.098	0.021
2-1, 119	7.39	−0.026	0.339	0.120	0.54	0.035	0.043	36.4	0.023	0.25	1.81	0.098	0.025
2-1, 129	7.49	−0.023	0.340	0.125	0.56	0.035	0.043	36.7	0.023	0.25	1.83	0.097	0.024
2-1, 139	7.59	−0.040	0.343	0.122	0.54	0.035	0.042	36.9	0.024	0.25	1.79	0.100	0.026
2-1, 149	7.69	0.148	0.357	0.143	0.58	0.044	0.039	36.3	0.025	0.33	2.43	0.101	0.016
2-2, 9	7.79	−0.028	0.363	0.149	0.58	0.045	0.041	35.6	0.025	0.37	2.77	0.099	0.026
2-2, 19	7.89	0.109	0.359	0.141	0.57	0.044	0.042	35.8	0.025	0.36	2.69	0.098	0.024
2-2, 29	7.99	0.229	0.340	0.153	0.60	0.048	0.040	36.3	0.025	0.38	2.80	0.096	0.035
2-2, 39	8.09	0.018	0.373	0.167	0.62	0.052	0.041	36.0	0.027	0.44	3.37	0.101	0.023
2-2, 49	8.19	0.167	0.350	0.149	0.58	0.047	0.038	35.7	0.025	0.39	2.95	0.097	0.020
2-2, 59	8.29	0.152	0.365	0.166	0.63	0.054	0.039	35.5	0.026	0.42	3.23	0.100	0.020
2-2, 69	8.39	0.170	0.365	0.166	0.62	0.051	0.040	35.4	0.026	0.44	3.34	0.098	0.022
2-2, 79	8.49	0.242	0.392	0.163	0.61	0.050	0.037	36.1	0.026	0.40	2.99	0.099	0.017
2-2, 89	8.59	0.149	0.356	0.155	0.59	0.049	0.040	35.4	0.026	0.42	3.20	0.096	0.020
2-2, 99	8.69	0.181	0.360	0.161	0.60	0.050	0.038	35.7	0.025	0.43	3.29	0.098	0.022
2-2, 109	8.79	0.204	0.374	0.162	0.61	0.050	0.038	35.6	0.025	0.42	3.21	0.098	0.020
2-2, 119	8.89	0.286	0.383	0.171	0.63	0.054	0.039	35.8	0.026	0.43	3.32	0.098	0.016
2-2, 129	8.99	0.166	0.363	0.166	0.61	0.051	0.042	35.1	0.026	0.44	3.37	0.097	0.023
2-2, 139	9.09	0.166	0.369	0.162	0.60	0.050	0.038	35.9	0.026	0.43	3.28	0.098	0.019
2-3, 9	9.29	0.149	0.368	0.160	0.60	0.050	0.040	35.8	0.026	0.43	3.29	0.097	0.023
2-3, 19	9.39	0.191	0.374	0.172	0.63	0.053	0.040	35.4	0.026	0.45	3.40	0.102	0.023
2-3, 29	9.49	0.128	0.370	0.158	0.61	0.049	0.039	35.8	0.026	0.43	3.28	0.098	0.021
2-3, 39	9.59	0.127	0.383	0.159	0.61	0.049	0.040	35.4	0.025	0.40	3.02	0.099	0.022
2-3, 49	9.69	0.113	0.382	0.167	0.62	0.051	0.044	35.2	0.026	0.43	3.29	0.104	0.028
2-3, 69	9.89	0.067	0.430	0.201	0.74	0.063	0.046	34.7	0.029	0.62	4.44	0.101	0.028
2-3, 79	9.99	0.150	0.400	0.178	0.69	0.059	0.040	34.9	0.027	0.63	4.22	0.100	0.026
2-3, 89	10.09	0.258	0.363	0.153	0.60	0.049	0.037	35.9	0.024	0.39	2.89	0.100	0.015
2-3, 99	10.19	0.175	0.365	0.161	0.62	0.052	0.039	35.2	0.026	0.49	3.54	0.098	0.025
2-3, 109	10.29	0.200	0.385	0.173	0.68	0.057	0.037	35.1	0.027	0.60	4.08	0.099	0.019
2-3, 119	10.39	0.236	0.394	0.190	0.73	0.063	0.039	34.6	0.029	0.74	4.82	0.100	0.026
2-3, 129	10.49	0.056	0.420	0.188	0.73	0.062	0.043	34.9	0.028	0.68	4.54	0.098	0.030
2-3, 139	10.59	0.208	0.430	0.205	0.77	0.069	0.043	34.1	0.029	0.77	4.99	0.104	0.026
2-3, 149	10.69	0.092	0.453	0.214	0.81	0.073	0.044	34.1	0.030	0.83	5.38	0.103	0.035
2-4, 9	10.79	0.221	0.424	0.208	0.79	0.071	0.044	33.7	0.029	0.79	5.25	0.103	0.027
2-4, 19	10.89	0.093	0.494	0.246	0.92	0.083	0.047	33.2	0.031	0.93	6.14	0.106	0.031
2-4, 39	10.99	0.142	0.480	0.228	0.84	0.072	0.041	34.2	0.030	0.79	5.20	0.101	0.030
2-4, 39	11.09	0.213	0.401	0.194	0.74	0.067	0.041	34.5	0.029	0.69	4.71	0.102	0.025
2-4, 59	11.29	0.219	0.392	0.196	0.78	0.072	0.043	33.4	0.030	0.83	5.57	0.099	0.044
2-4, 69	11.39	0.065	0.486	0.237	0.92	0.083	0.048	33.0	0.032	0.96	6.45	0.097	0.034
2-4, 79	11.49	0.221	0.435	0.211	0.80	0.070	0.041	33.7	0.030	0.80	5.46	0.093	0.027
2-4, 89	11.59	0.216	0.461	0.228	0.87	0.077	0.044	33.7	0.031	0.89	5.98	0.099	0.027
2-4, 99	11.69	0.039	0.459	0.226	0.88	0.079	0.047	33.2	0.033	0.96	6.57	0.091	0.052
2-4, 109	11.79	0.235	0.480	0.227	0.88	0.076	0.042	33.1	0.031	0.92	6.24	0.093	0.022
2-4, 119	11.89	0.228	0.475	0.225	0.87	0.071	0.044	33.9	0.031	0.89	5.76	0.091	0.030
2-4, 129	11.99	0.220	0.447	0.212	0.84	0.071	0.046	33.9	0.031	0.90	5.98	0.089	0.031
2-4, 139	12.09	0.233	0.511	0.257	0.97	0.084	0.047	32.4	0.034	1.02	7.01	0.097	0.023
2-5, 9	12.29	0.222	0.494	0.250	0.97	0.083	0.049	32.9	0.033	1.01	6.79	0.097	0.034
2-5, 19	12.39	0.087	0.491	0.238	0.92	0.080	0.048	33.1	0.032	0.98	6.54	0.093	0.030
2-5, 29	12.49	0.099	0.489	0.247	0.94	0.082	0.048	32.4	0.033	1.01	6.84	0.093	0.028

Table 1 (continued).

Core-Section (level in cm)	Sub-bottom depth (m)	Na	Mg	Al	Si	P	K	Ca	Ti	Mn	Fe	Ba	S
Site 598 (Cont.)													
2-5, 39	12.59	0.126	0.578	0.300	1.13	0.104	0.056	31.2	0.036	1.18	8.22	0.106	0.034
2-5, 49	12.69	0.118	0.567	0.293	1.11	0.101	0.054	31.6	0.036	1.18	8.09	0.103	0.032
2-5, 59	12.79	0.103	0.592	0.302	1.13	0.103	0.056	31.9	0.036	1.19	8.15	0.099	0.033
2-5, 69	12.89	0.135	0.480	0.251	0.98	0.091	0.053	31.9	0.033	1.20	7.75	0.089	0.051
2-5, 89	13.09	0.053	0.527	0.277	1.07	0.097	0.052	31.2	0.034	1.15	7.86	0.093	0.060
2-5, 109	13.29	0.223	0.581	0.313	1.15	0.102	0.055	31.4	0.035	1.21	8.03	0.096	0.036
2-5, 130	13.50	0.083	0.497	0.241	0.94	0.089	0.048	32.3	0.032	1.02	7.06	0.091	0.027
2-5, 139	13.59	0.213	0.536	0.250	0.96	0.086	0.045	32.4	0.032	1.04	7.02	0.088	0.024
2-5, 149	13.69	0.075	0.557	0.254	0.97	0.089	0.052	33.1	0.032	1.07	7.07	0.088	0.032
2-6, 9	13.79	0.101	0.526	0.244	0.94	0.084	0.047	32.4	0.031	1.03	6.79	0.086	0.027
2-6, 19	13.89	0.108	0.484	0.230	0.91	0.087	0.043	32.2	0.032	1.04	6.87	0.084	0.048
2-6, 29	13.99	0.090	0.523	0.240	0.93	0.085	0.047	32.8	0.031	1.02	6.81	0.084	0.028
2-6, 39	14.09	0.099	0.503	0.234	0.91	0.080	0.047	32.0	0.031	1.01	6.76	0.086	0.028
2-6, 49	14.19	0.103	0.532	0.240	0.93	0.082	0.046	32.8	0.031	1.02	6.75	0.086	0.027
2-6, 59	14.29	0.039	0.515	0.238	0.92	0.080	0.048	33.1	0.031	1.02	6.74	0.086	0.030
2-6, 69	14.39	0.229	0.516	0.248	0.96	0.085	0.046	32.8	0.032	1.04	6.77	0.088	0.030
2-6, 79	14.49	0.072	0.493	0.239	0.93	0.083	0.049	32.6	0.033	1.04	6.69	0.084	0.049
2-6, 89	14.59	0.086	0.539	0.298	1.11	0.102	0.058	31.3	0.037	1.28	7.98	0.089	0.057
2-6, 99	14.69	0.043	0.517	0.268	1.01	0.092	0.055	32.0	0.035	1.16	7.46	0.087	0.054
2-6, 119	14.89	0.240	0.520	0.256	0.98	0.088	0.050	32.3	0.033	1.08	6.99	0.085	0.036
2-6, 139	15.09	0.243	0.532	0.264	0.99	0.086	0.049	32.6	0.033	1.08	6.87	0.084	0.028
2-6, 149	15.19	0.228	0.552	0.263	0.99	0.087	0.050	32.8	0.033	1.07	6.72	0.085	0.031
3-1, 9	15.89	0.232	0.692	0.345	1.41	0.130	0.064	28.9	0.041	1.74	10.45	0.103	0.033
3-1, 19	15.99	0.233	0.572	0.286	1.24	0.117	0.059	28.5	0.039	1.71	10.24	0.097	0.052
3-1, 29	16.09	0.185	0.693	0.345	1.41	0.132	0.066	28.3	0.041	1.77	10.60	0.102	0.034
3-1, 39	16.19	0.272	0.666	0.337	1.42	0.134	0.065	27.6	0.043	1.82	10.98	0.101	0.035
3-1, 49	16.29	0.153	0.702	0.342	1.41	0.133	0.068	28.6	0.042	1.79	10.70	0.101	0.037
3-1, 59	16.39	0.154	0.702	0.344	1.41	0.131	0.066	28.4	0.042	1.78	10.63	0.104	0.033
3-1, 69	16.49	0.153	0.677	0.315	1.32	0.126	0.063	29.5	0.041	1.72	10.15	0.100	0.034
3-1, 79	16.59	0.074	0.517	0.214	0.97	0.093	0.048	31.8	0.035	1.29	7.61	0.091	0.055
3-1, 89	16.69	0.255	0.688	0.332	1.39	0.127	0.063	28.9	0.041	1.65	10.29	0.103	0.036
3-1, 99	16.79	0.086	0.597	0.292	1.24	0.119	0.060	29.6	0.039	1.57	9.58	0.097	0.061
3-1, 109	16.89	0.179	0.475	0.186	0.87	0.086	0.044	32.3	0.031	1.27	7.17	0.091	0.047
3-1, 119	16.99	0.137	0.560	0.243	1.02	0.095	0.051	31.9	0.034	1.28	7.70	0.092	0.028
3-1, 129	17.09	0.098	0.556	0.193	0.89	0.087	0.050	32.7	0.030	1.25	6.87	0.093	0.032
3-1, 139	17.19	0.230	0.509	0.188	0.86	0.082	0.044	32.9	0.030	1.17	6.42	0.093	0.032
3-1, 149	17.29	0.141	0.527	0.185	0.87	0.083	0.045	33.0	0.030	1.22	6.67	0.093	0.028
3-2, 9	17.39	0.086	0.470	0.170	0.81	0.080	0.043	33.0	0.030	1.15	6.27	0.092	0.047
3-2, 19	17.49	0.120	0.509	0.185	0.84	0.082	0.043	33.1	0.030	1.15	6.31	0.092	0.027
3-2, 31	17.61	0.299	0.524	0.201	0.89	0.083	0.042	32.8	0.030	1.17	6.33	0.095	0.031
3-2, 39	17.69	0.271	0.550	0.203	0.91	0.085	0.043	32.9	0.030	1.21	6.38	0.095	0.031
3-2, 49	17.79	0.057	0.487	0.171	0.82	0.081	0.043	33.2	0.030	1.17	6.30	0.095	0.054
3-2, 59	17.89	0.148	0.489	0.177	0.82	0.080	0.043	33.1	0.029	1.15	6.25	0.091	0.026
3-2, 69	17.99	0.110	0.509	0.205	0.87	0.082	0.044	33.4	0.031	1.12	6.35	0.093	0.025
3-2, 79	18.09	0.062	0.483	0.193	0.85	0.082	0.050	32.9	0.031	1.12	6.46	0.095	0.051
3-2, 89	18.19	0.079	0.474	0.196	0.86	0.082	0.046	32.7	0.030	1.11	6.50	0.095	0.048
3-2, 99	18.29	0.221	0.447	0.163	0.78	0.075	0.035	32.3	0.028	1.16	6.27	0.087	0.038
3-2, 109	18.39	0.253	0.469	0.182	0.82	0.078	0.042	33.2	0.030	1.11	6.12	0.092	0.029
3-2, 119	18.49	0.220	0.510	0.198	0.88	0.081	0.042	31.9	0.031	1.16	6.25	0.090	0.029
3-2, 129	18.59	0.226	0.431	0.148	0.72	0.070	0.037	33.8	0.028	1.15	5.90	0.080	0.041
3-3, 9	18.89	0.268	0.505	0.148	0.76	0.072	0.038	33.1	0.029	1.45	5.69	0.075	0.026
3-3, 19	18.99	0.145	0.497	0.146	0.74	0.071	0.038	32.5	0.028	1.32	5.85	0.074	0.024
3-3, 29	19.09	0.024	0.484	0.197	0.88	0.083	0.045	32.4	0.032	1.23	6.83	0.088	0.052
3-3, 39	19.19	0.088	0.490	0.133	0.72	0.075	0.039	33.3	0.027	1.42	5.86	0.077	0.048
3-3, 49	19.29	0.152	0.498	01.36	0.67	0.061	0.039	34.3	0.026	1.21	4.95	0.074	0.024
3-3, 59	19.39	0.100	0.520	0.144	0.78	0.077	0.044	32.4	0.027	1.63	6.53	0.075	0.050
3-3, 69	19.49	0.188	0.521	0.125	0.71	0.071	0.039	33.1	0.025	1.44	5.85	0.071	0.024
3-3, 79	19.59	0.169	0.524	0.116	0.66	0.067	0.036	33.4	0.026	1.42	5.50	0.064	0.023
3-3, 89	19.69	0.159	0.455	0.112	0.64	0.064	0.036	33.2	0.025	1.26	5.35	0.069	0.040
3-3, 99	19.79	0.236	0.482	0.118	0.65	0.064	0.034	33.6	0.026	1.32	4.87	0.068	0.025
3-3, 109	19.89	0.259	0.466	0.122	0.67	0.065	0.038	33.2	0.026	1.45	5.15	0.068	0.026
3-3, 119	19.99	0.067	0.501	0.116	0.69	0.074	0.036	33.0	0.026	1.52	6.01	0.072	0.049
3-3, 129	20.09	0.174	0.489	0.108	0.65	0.067	0.039	34.0	0.024	1.56	5.71	0.067	0.023
3-3, 139	20.19	0.078	0.427	0.095	0.57	0.057	0.035	34.2	0.023	1.32	4.63	0.069	0.023
3-3, 149	20.29	0.268	0.450	0.112	0.62	0.063	0.031	34.0	0.025	1.31	4.52	0.065	0.020
3-4, 9	20.39	0.059	0.467	0.095	0.60	0.064	0.039	34.1	0.024	1.41	4.84	0.067	0.048
3-4, 19	20.49	0.189	0.475	0.110	0.65	0.065	0.035	33.1	0.025	1.46	4.94	0.069	0.026
3-4, 29	20.59	0.085	0.424	0.086	0.54	0.054	0.033	34.1	0.023	1.25	4.44	0.062	0.040
3-4, 39	20.69	0.086	0.491	0.095	0.59	0.059	0.041	34.6	0.025	1.32	4.61	0.066	0.030
3-4, 49	20.79	0.130	0.452	0.097	0.59	0.058	0.035	34.5	0.025	1.26	4.49	0.069	0.022
3-4, 59	20.89	0.161	0.485	0.108	0.67	0.066	0.036	33.4	0.024	1.39	5.71	0.066	0.023
3-4, 69	20.99	0.145	0.432	0.091	0.57	0.058	0.035	34.5	0.024	1,42	4.46	0.067	0.021
3-4, 79	21.09	0.045	0.433	0.099	0.61	0.063	0.038	33.8	0.024	1.40	4.93	0.069	0.044
3-4, 89	21.19	0.180	0.417	0.100	0.63	0.062	0.036	33.4	0.025	1.39	5.11	0.063	0.026
3-4, 99	21.29	0.105	0.474	0.105	0.62	0.071	0.038	34.1	0.026	1.42	4.68	0.068	0.025

Table 1 (continued).

Core-Section (level in cm)	Sub-bottom depth (m)	Na	Mg	Al	Si	P	K	Ca	Ti	Mn	Fe	Ba	S
Site 598 (Cont.)													
3-4, 109	21.39	0.071	0.409	0.092	0.58	0.065	0.034	33.9	0.024	1.34	4.72	0.071	0.046
3-4, 119	21.49	0.065	0.440	0.093	0.58	0.059	0.038	34.3	0.024	1.38	4.60	0.065	0.046
3-4, 129	21.59	0.035	0.404	0.089	0.55	0.055	0.036	33.5	0.023	1.24	4.34	0.064	0.044
3-4, 139	21.69	0.235	0.381	0.092	0.55	0.058	0.030	34.2	0.024	1.24	4.32	0.064	0.021
3-5, 1	21.81	0.143	0.422	0.093	0.57	0.078	0.035	34.4	0.024	1.39	4.57	0.067	0.022
3-5, 19	21.99	0.065	0.416	0.086	0.56	0.058	0.034	35.2	0.024	1.32	4.47	0.066	0.022
3-5, 29	22.09	0.089	0.461	0.093	0.65	0.065	0.038	33.2	0.023	1.62	5.63	0.066	0.046
3-5, 39	22.19	0.244	0.488	0.104	0.69	0.074	0.040	32.7	0.024	1.78	5.88	0.068	0.028
3-5, 49	22.29	0.246	0.536	0.124	0.76	0.085	0.041	32.5	0.027	1.85	6.18	0.075	0.029
3-5, 59	22.39	0.209	0.539	0.113	0.77	0.089	0.041	31.5	0.026	2.07	7.06	0.074	0.049
3-5, 69	22.49	0.165	0.593	0.117	0.75	0.084	0.045	33.0	0.025	1.82	6.00	0.070	0.029
3-5, 79	22.59	0.126	0.510	0.120	0.78	0.089	0.044	31.9	0.026	2.04	6.77	0.072	0.049
3-5, 89	22.69	0.121	0.570	0.136	0.86	0.097	0.046	31.2	0.028	2.32	7.63	0.076	0.051
3-5, 99	22.79	0.240	0.517	0.133	0.77	0.095	0.042	32.3	0.028	1.90	6.13	0.073	0.029
3-5, 109	22.89	0.110	0.539	0.133	0.82	0.102	0.047	31.7	0.030	2.23	6.98	0.074	0.054
3-5, 119	22.99	0.215	0.559	0.130	0.80	0.104	0.046	32.0	0.028	2.14	6.77	0.074	0.028
3-5, 129	23.09	0.178	0.572	0.119	0.77	0.088	0.045	32.3	0.025	2.01	6.67	0.069	0.028
3-5, 139	23.19	0.159	0.505	0.108	0.69	0.080	0.042	32.9	0.025	1.98	5.75	0.069	0.026
3-5, 149	23.29	0.294	0.443	0.096	0.63	0.071	0.036	33.1	0.024	1.77	5.30	0.065	0.023
3-6, 9	23.39	0.077	0.484	0.098	0.67	0.073	0.037	32.9	0.024	1.86	5.83	0.067	0.051
3-6, 19	23.49	0.176	0.482	0.102	0.67	0.075	0.039	32.9	0.024	1.87	5.91	0.066	0.023
3-6, 39	23.69	0.214	0.532	0.107	0.69	0.077	0.039	33.1	0.023	1.83	5.61	0.066	0.025
3-6, 49	23.79	0.183	0.483	0.099	0.63	0.072	0.038	33.8	0.024	1.78	5.21	0.067	0.021
3-6, 59	23.89	0.125	0.477	0.104	0.68	0.074	0.040	33.0	0.025	1.92	5.57	0.068	0.047
3-6, 69	23.99	0.218	0.582	0.122	0.79	0.081	0.046	31.9	0.025	2.20	6.65	0.069	0.029
3-6, 89	24.19	0.149	0.552	0.132	0.83	0.088	0.053	31.4	0.027	2.44	7.19	0.073	0.031
3-6, 99	24.29	0.209	0.596	0.158	0.95	0.111	0.049	30.9	0.029	2.50	7.30	0.074	0.034
3-6, 109	24.39	0.096	0.562	0.132	0.90	0.110	0.054	30.5	0.027	2.71	8.07	0.076	0.057
3-6, 119	24.49	0.165	0.624	0.133	0.92	0.103	0.052	30.1	0.026	2.57	8.37	0.072	0.030
4-1, 9	25.59	0.191	0.557	0.131	0.90	0.100	0.054	29.7	0.026	2.88	8.07	0.074	0.049
4-1, 49	25.89	0.108	0.572	0.132	0.92	0.105	0.056	29.8	0.027	2.95	7.86	0.074	0.061
4-1, 59	25.99	0.156	0.638	0.161	1.06	0.124	0.058	28.7	0.030	3.34	9.03	0.079	0.065
4-1, 69	26.09	0.196	0.749	0.206	1.34	0.151	0.074	26.1	0.032	4.12	11.33	0.086	0.074
4-1, 89	26.29	0.337	0.855	0.230	1.38	0.176	0.079	26.1	0.036	4.30	10.90	0.090	0.039
4-1, 99	26.39	0.302	0.746	0.176	1.13	0.144	0.066	28.2	0.030	3.61	9.38	0.080	0.034
4-1, 110	26.50	0.129	0.593	0.140	0.92	0.120	0.052	30.0	0.029	3.01	7.85	0.079	0.062
4-1, 119	26.59	0.225	0.618	0.141	0.91	0.114	0.053	30.5	0.029	2.98	7.58	0.077	0.030
4-1, 139	26.79	0.260	0.754	0.168	1.10	0.116	0.065	28.3	0.029	3.58	9.31	0.079	0.063
4-1, 149	26.89	0.269	0.747	0.182	1.11	0.105	0.061	29.1	0.031	3.18	9.01	0.075	0.034
4-2, 9	26.99	0.093	0.526	0.116	0.72	0.087	0.050	32.6	0.026	2.20	5.79	0.068	0.032
4-2, 19	27.09	0.157	0.551	0.129	0.80	0.104	0.050	31.7	0.027	2.49	6.40	0.071	0.030
4-2, 29	27.19	0.171	0.549	0.130	0.80	0.094	0.051	31.9	0.028	2.43	6.33	0.071	0.029
4-2, 39	27.29	0.172	0.564	0.136	0.85	0.114	0.053	31.6	0.027	2.57	6.77	0.074	0.056
4-2, 49	27.39	0.132	0.555	0.133	0.80	0.109	0.052	32.4	0.026	2.26	6.16	0.071	0.032
4-2, 59	27.49	0.139	0.523	0.140	0.81	0.093	0.048	31.7	0.029	2.48	6.54	0.073	0.028
4-2, 69	27.59	0.136	0.425	0.108	0.64	0.099	0.040	33.0	0.027	1.87	5.00	0.067	0.026
4-2, 99	27.89	0.138	0.499	0.116	0.74	0.134	0.044	32.7	0.027	2.08	6.06	0.070	0.028
4-2, 109	27.99	0.157	0.551	0.111	0.70	0.126	0.041	33.7	0.025	1.69	5.20	0.065	0.037
4-2, 119	28.09	0.113	0.528	0.119	0.76	0.089	0.050	32.6	0.028	2.23	6.12	0.070	0.055
4-2, 129	28.19	0.229	0.565	0.128	0.79	0.087	0.046	32.2	0.027	2.19	6.19	0.074	0.051
4-2, 139	28.29	0.205	0.601	0.138	0.89	0.089	0.052	30.8	0.027	2.64	7.43	0.075	0.055
4-3, 9	28.49	0.131	0.519	0.125	0.85	0.079	0.053	30.2	0.027	2.74	7.50	0.078	0.049
4-3, 30	28.70	0.066	0.506	0.127	0.82	0.084	0.051	30.9	0.027	2.49	7.15	0.073	0.056
4-3, 39	28.79	0.115	0.520	0.122	0.84	0.088	0.049	30.9	0.028	2.86	7.62	0.077	0.051
4-3, 49	28.89	0.042	0.532	0.121	0.83	0.099	0.050	31.0	0.027	2.67	7.50	0.074	0.057
4-3, 69	29.09	0.173	0.546	0.119	0.82	0.153	0.046	31.2	0.026	2.63	7.30	0.071	0.051
4-3, 89	29.29	0.084	0.563	0.142	0.90	0.117	0.058	30.8	0.029	2.77	7.33	0.076	0.063
4-3, 99	29.39	0.104	0.631	0.168	1.03	0.116	0.063	29.1	0.031	3.27	8.51	0.078	0.065
4-3, 109	29.49	0.163	0.510	0.112	0.68	0.077	0.042	33.3	0.026	1.87	5.31	0.066	0.028
4-3, 119	29.59	0.170	0.647	0.175	1.02	0.101	0.065	30.7	0.031	2.91	7.93	0.075	0.036
4-3, 129	29.69	0.268	0.577	0.164	0.93	0.096	0.054	31.7	0.030	2.48	6.81	0.077	0.026
4-3, 139	29.79	0.120	0.471	0.135	0.77	0.085	0.048	32.5	0.028	2.05	5.99	0.071	0.052
4-3, 149	29.89	0.052	0.526	0.146	0.84	0.092	0.050	31.6	0.029	2.25	6.84	0.071	0.055
4-4, 9	29.99	0.177	0.493	0.125	0.77	0.078	0.045	31.7	0.027	2.24	6.39	0.071	0.047
4-4, 30	30.20	0.049	0.494	0.133	0.73	0.081	0.043	32.1	0.030	2.01	6.12	0.069	0.053
4-4, 39	30.29	0.418	0.454	0.123	0.73	0.097	0.039	33.1	0.028	1.95	5.83	0.068	0.045
4-4, 49	30.39	0.204	0.459	0.117	0.71	0.097	0.039	32.5	0.027	2.03	5.88	0.068	0.044
4-4, 59	30.49	0.089	0.489	0.111	0.69	0.091	0.043	32.5	0.027	1.94	5.66	0.066	0.050
4-4, 69	30.59	0.170	0.526	0.107	0.69	0.068	0.042	33.4	0.025	1.87	5.57	0.065	0.026
4-4, 79	30.69	0.156	0.530	0.106	0.69	0.067	0.042	33.4	0.026	1.87	5.57	0.065	0.026
4-4, 89	30.79	0.153	0.464	0.101	0.64	0.085	0.039	32.7	0.026	1.87	5.20	0.061	0.046
4-4, 119	31.09	0.144	0.561	0.140	0.79	0.079	0.043	32.5	0.029	1.98	5.92	0.065	0.044
4-4, 130	31.20	0.072	0.523	0.114	0.73	0.082	0.043	32.6	0.026	1.97	6.23	0.067	0.051
4-4, 139	31.29	0.147	0.463	0.088	0.58	0.068	0.040	33.3	0.023	1.79	4.92	0.061	0.043
4-5, 9	31.49	0.074	0.439	0.077	0.53	0.062	0.032	34.8	0.023	1.39	4.28	0.061	0.044

Table 1 (continued).

Core-Section (level in cm)	Sub-bottom depth (m)	Na	Mg	Al	Si	P	K	Ca	Ti	Mn	Fe	Ba	S
Site 598 (Cont.)													
4-5, 19	31.59	0.142	0.486	0.087	0.57	0.068	0.036	34.7	0.023	1.42	4.36	0.060	0.023
4-5, 29	31.69	0.148	0.546	0.092	0.62	0.075	0.035	33.7	0.023	1.77	5.12	0.063	0.023
4-5, 39	31.79	0.177	0.510	0.087	0.60	0.076	0.038	33.8	0.023	1.59	4.88	0.063	0.025
4-5, 49	31.89	0.154	0.640	0.119	0.86	0.086	0.054	30.9	0.024	2.44	7.94	0.070	0.034
4-5, 59	31.99	0.238	0.689	0.139	0.90	0.099	0.055	30.6	0.025	2.73	7.88	0.074	0.035
4-5, 69	32.09	0.203	0.624	0.149	0.90	0.086	0.056	31.6	0.026	2.61	6.95	0.075	0.030
4-5, 81	32.20	0.269	0.770	0.249	1.22	0.122	0.064	29.6	0.036	3.06	8.02	0.082	0.035
4-5, 89	32.29	0.180	0.622	0.165	0.89	0.104	0.047	32.0	0.029	2.29	6.35	0.076	0.030
4-5, 99	32.39	0.116	0.544	0.120	0.71	0.091	0.042	33.2	0.025	1.90	5.59	0.069	0.027
4-5, 110	32.49	0.220	0.585	0.127	0.77	0.084	0.046	32.6	0.026	2.09	6.03	0.070	0.029
4-5, 118	32.58	0.167	0.586	0.123	0.77	0.092	0.048	32.4	0.025	2.07	6.16	0.067	0.031
4-6, 9	32.99	0.234	0.790	0.209	1.26	0.129	0.068	27.4	0.032	3.26	10.57	0.087	0.038
4-6, 20	33.10	0.272	0.817	0.157	1.20	0.132	0.061	27.5	0.027	3.46	10.79	0.084	0.032
4-6, 30	33.20	0.286	0.834	0.159	1.21	0.143	0.067	26.8	0.026	3.66	11.00	0.083	0.038
5-1, 9	35.09	0.256	0.634	0.111	0.89	0.102	0.053	30.0	0.023	2.80	8.19	0.071	0.032
5-1, 19	35.19	0.193	0.567	0.098	0.75	0.116	0.046	31.5	0.023	2.29	6.76	0.067	0.032
5-1, 29	35.29	0.211	0.588	0.105	0.81	0.094	0.049	31.1	0.023	2.46	7.24	0.070	0.030
5-1, 39	35.39	0.181	0.712	0.122	1.01	0.153	0.053	28.9	0.026	3.18	9.44	0.074	0.032
5-1, 49	35.49	0.190	0.752	0.127	1.07	0.118	0.054	28.4	0.023	2.83	10.32	0.074	0.033
5-1, 59	35.59	0.243	0.674	0.127	0.96	0.199	0.055	29.7	0.026	3.05	8.51	0.076	0.042
5-1, 69	35.69	0.216	0.675	0.150	1.05	0.171	0.054	29.2	0.026	3.09	9.00	0.080	0.040
5-1, 80	35.80	0.231	0.703	0.154	1.07	0.152	0.062	29.0	0.027	3.29	9.09	0.089	0.039
5-1, 89	35.89	0.253	0.834	0.168	1.26	0.128	0.070	26.2	0.026	3.76	11.56	0.085	0.040
5-1, 99	35.99	0.225	0.679	0.136	0.99	0.153	0.055	29.1	0.026	3.30	8.52	0.081	0.040
5-1, 109	36.09	0.233	0.659	0.144	0.98	0.152	0.055	29.9	0.026	3.18	8.16	0.080	0.044
5-1, 119	36.19	0.262	0.786	0.145	1.13	0.135	0.063	27.7	0.024	3.52	10.38	0.085	0.039
5-1, 129	36.30	0.132	0.662	0.137	0.93	0.114	0.057	30.0	0.025	2.86	8.13	0.080	0.034
5-1, 142	36.42	0.186	0.640	0.131	0.88	0.103	0.056	31.3	0.025	2.51	7.26	0.079	0.033
5-2, 9	36.59	0.293	0.693	0.123	0.92	0.112	0.054	30.4	0.024	2.85	8.00	0.079	0.035
5-2, 19	36.69	0.347	0.822	0.162	1.24	0.118	0.068	26.2	0.025	3.89	11.30	0.088	0.039
5-2, 31	36.81	0.224	0.696	0.151	1.05	0.136	0.059	29.3	0.027	3.33	8.80	0.087	0.037
5-2, 39	36.89	0.249	0.660	0.127	0.87	0.099	0.050	31.2	0.025	2.71	7.06	0.074	0.033
5-2, 49	36.99	0.446	0.805	0.148	1.14	0.171	0.062	27.5	0.024	3.31	10.01	0.077	0.035
5-2, 59	37.09	0.223	0.437	0.090	0.61	0.314	0.037	33.8	0.024	1.36	4.96	0.066	0.043
5-2, 71	37.21	0.414	0.923	0.159	1.34	0.121	0.069	24.1	0.025	4.38	12.68	0.085	0.036
5-2, 79	37.29	0.272	0.776	0.153	1.12	0.126	0.058	28.4	0.026	3.50	9.59	0.082	0.034
5-2, 89	37.39	0.331	0.775	0.146	1.14	0.127	0.063	27.1	0.025	3.79	10.06	0.083	0.036
5-2, 99	37.49	0.320	0.787	0.161	1.17	0.120	0.065	26.6	0.027	3.81	10.57	0.084	0.032
5-2, 109	37.59	0.275	0.713	0.151	1.03	0.125	0.060	29.1	0.027	3.15	8.77	0.086	0.037
5-2, 119	37.69	0.314	0.827	0.172	1.29	0.126	0.066	26.1	0.025	3.98	11.48	0.086	0.038
5-2, 129	37.79	0.289	0.841	0.201	1.34	0.126	0.070	25.4	0.028	3.95	11.79	0.088	0.041
5-2, 139	37.89	0.317	0.710	0.162	1.06	0.126	0.060	28.4	0.027	3.29	9.05	0.082	0.038
5-3, 9	38.09	0.245	0.682	0.140	1.00	0.117	0.056	29.4	0.025	3.08	8.91	0.077	0.036
5-3, 19	38.19	0.296	0.664	0.129	0.97	0.100	0.054	30.1	0.024	3.16	8.55	0.080	0.037
5-3, 29	38.29	0.272	0.602	0.122	0.81	0.101	0.049	31.5	0.025	2.65	6.70	0.073	0.032
5-3, 39	38.39	0.197	0.613	0.134	0.89	0.084	0.054	30.7	0.026	2.86	7.32	0.081	0.032
5-3, 49	38.49	0.373	0.668	0.159	1.04	0.09	0.058	28.8	0.027	3.13	8.94	0.082	0.032
5-3, 59	38.59	0.270	0.582	0.123	0.84	0.95	0.049	31.9	0.024	2.39	6.81	0.078	0.032
5-3, 79	38.79	0.266	0.715	0.205	1.25	0.13	0.068	28.0	0.031	3.45	9.60	0.105	0.040
5-3, 99	38.99	0.278	0.808	0.208	1.37	0.06	0.076	26.0	0.029	3.90	11.03	0.101	0.044
5-3, 109	39.09	0.398	0.797	0.182	1.30	0.03	0.075	25.6	0.028	4.03	11.23	0.096	0.047
5-3, 119	39.19	0.240	0.622	0.151	1.03	0.96	0.059	29.6	0.027	2.92	8.68	0.091	0.036
5-3, 129	39.29	0.300	0.703	0.152	1.08	0.11	0.057	28.7	0.027	3.13	9.32	0.084	0.048
5-3, 139	39.39	0.209	0.711	0.141	1.05	0.21	0.060	29.5	0.027	2.97	8.99	0.088	0.041
5-3, 149	39.49	0.422	0.810	0.165	1.24	0.44	0.071	26.1	0.027	3.92	10.82	0.097	0.051
5-4, 9	39.59	0.196	0.846	0.224	1.50	0.62	0.083	24.8	0.031	4.48	12.17	0.106	0.056
5-4, 19	39.69	0.298	0.800	0.208	1.31	0.50	0.073	27.7	0.031	3.53	10.12	0.101	0.044
5-4, 29	39.79	0.320	0.830	0.188	1.29	0.45	0.071	26.1	0.030	3.73	11.54	0.084	0.045
5-4, 39	39.89	0.319	0.760	0.148	1.10	0.36	0.062	28.6	0.025	3.05	9.65	0.079	0.039
5-4, 49	39.99	0.368	0.804	0.159	1.19	0.70	0.063	27.2	0.027	3.66	10.38	0.080	0.038
5-4, 59	40.09	0.306	0.759	0.142	1.16	0.71	0.058	27.5	0.025	3.38	10.76	0.078	0.040
5-4, 69	40.19	0.239	0.723	0.149	1.04	0.25	0.054	30.3	0.029	2.74	8.27	0.077	0.038
5-4, 79	40.29	0.239	0.670	0.124	0.94	0.47	0.054	30.1	0.025	2.71	8.23	0.081	0.038
5-4, 89	40.39	0.175	0.647	0.145	1.03	0.26	0.060	29.5	0.026	2.86	9.15	0.085	0.039
5-4, 99	40.49	0.366	0.858	0.176	1.43	0.33	0.073	23.7	0.027	4.30	12.85	0.097	0.048
5-4, 139	40.89	0.332	0.764	0.155	1.15	0.73	0.066	27.9	0.028	3.48	9.76	0.085	0.061
5-5, 9	41.09	0.288	0.699	0.132	0.97	0.42	0.057	30.0	0.026	3.00	8.22	0.082	0.038
5-5, 29	41.29	0.348	0.819	0.135	1.16	0.87	0.067	27.5	0.030	3.75	10.21	0.085	0.041
5-5, 39	41.39	0.338	0.802	0.167	1.27	0.50	0.063	26.9	0.028	4.04	10.74	0.096	0.035
5-5, 49	41.49	0.472	0.765	0.150	1.18	0.12	0.062	27.6	0.027	3.73	9.95	0.085	0.045
5-5, 59	41.59	0.356	0.807	0.169	1.26	0.26	0.076	27.3	0.028	4.02	10.26	0.093	0.046
5-5, 69	41.69	0.437	0.891	0.211	1.49	0.74	0.085	23.9	0.030	4.75	12.08	0.101	0.044
5-5, 89	41.89	0.380	0.912	0.191	1.46	0.37	0.080	24.1	0.028	4.22	12.70	0.089	0.045
5-5, 99	41.99	0.308	0.871	0.180	1.31	0.55	0.065	27.2	0.028	3.47	11.22	0.086	0.042
5-5, 109	42.09	0.286	0.740	0.166	1.15	0.77	0.065	28.6	0.028	3.15	9.28	0.081	0.042

Table 1 (continued).

Core-Section (level in cm)	Sub-bottom depth (m)	Na	Mg	Al	Si	P	K	Ca	Ti	Mn	Fe	Ba	S
Site 598 (Cont.)													
5-5, 119	42.19	0.478	0.671	0.149	1.00	0.60	0.053	29.7	0.027	2.75	8.17	0.073	0.026
5-5, 129	42.29	0.436	1.039	0.187	1.61	0.59	0.072	22.5	0.026	4.55	14.65	0.090	0.048
5-5, 139	42.39	0.225	0.671	0.133	0.93	0.85	0.054	30.8	0.028	2.66	7.64	0.079	0.040
5-5, 149	42.49	0.251	0.601	0.138	0.97	0.65	0.056	29.9	0.027	2.75	8.25	0.080	0.042
5-6, 19	42.69	0.292	0.779	0.187	1.26	0.89	0.070	28.1	0.030	3.20	9.80	0.085	0.042
5-6, 29	42.79	0.277	0.746	0.180	1.20	0.36	0.072	28.5	0.030	3.48	9.18	0.091	0.049
5-6, 41	42.91	0.251	0.732	0.169	1.12	0.03	0.064	29.4	0.029	3.08	9.05	0.077	0.042
5-6, 49	42.99	0.222	0.612	0.145	0.93	0.32	0.057	31.2	0.027	2.45	7.26	0.075	0.037
5-6, 59	43.09	0.259	0.794	0.220	1.27	0.15	0.063	29.1	0.034	2.80	9.19	0.079	0.040
5-6, 69	43.19	0.210	0.635	0.154	0.92	0.28	0.054	32.5	0.029	2.17	6.45	0.074	0.038
Site 599													
1-1, 129	1.29	0.262	0.345	0.323	0.90	0.081	0.079	35.7	0.037	0.43	2.57	0.111	0.026
1-2, 29	1.79	0.194	0.515	0.618	1.59	0.179	0.150	32.2	0.056	0.79	5.66	0.133	0.042
1-2, 129	2.79	0.093	0.357	0.214	0.66	0.089	0.045	34.9	0.028	0.47	3.56	0.098	0.026
1-3, 69	3.69	0.105	0.282	0.093	0.39	0.035	0.029	36.0	0.021	0.20	1.41	0.095	0.021
1-3, 89	3.89	−0.015	0.257	0.075	0.39	0.034	0.021	37.0	0.022	0.21	1.54	0.094	0.026
1-3, 129	4.29	0.001	0.282	0.073	0.41	0.038	0.020	36.6	0.023	0.31	2.15	0.092	0.029
1-4, 9	4.59	0.291	0.364	0.148	0.60	0.061	0.030	34.8	0.025	0.52	3.66	0.096	0.018
1-4, 29	4.79	0.040	0.299	0.101	0.53	0.052	0.021	35.8	0.024	0.47	3.24	0.106	0.027
1-4, 39	4.89	−0.008	0.329	0.110	0.57	0.059	0.026	35.5	0.025	0.52	3.64	0.099	0.030
1-4, 69	5.19	−0.002	0.318	0.100	0.55	0.052	0.025	35.4	0.025	0.54	3.48	0.098	0.030
1-4, 79	5.29	0.116	0.368	0.142	0.62	0.053	0.038	34.8	0.025	0.61	3.63	0.101	0.023
1-4, 89	5.39	0.005	0.354	0.119	0.65	0.062	0.029	35.0	0.025	0.74	4.61	0.104	0.034
1-5, 39	6.39	0.117	0.348	0.088	0.49	0.044	0.032	36.0	0.021	0.56	2.94	0.084	0.023
1-5, 127	7.27	0.181	0.352	0.085	0.50	0.047	0.022	36.1	0.022	0.57	3.09	0.087	0.021
1-6, 9	7.59	0.001	0.320	0.059	0.51	0.048	0.021	35.8	0.022	0.65	3.46	0.085	0.029
2-1, 59	8.49	0.122	0.466	0.107	0.80	0.068	0.047	34.3	0.023	1.28	5.52	0.095	0.029
2-1, 89	8.79	−0.012	0.298	0.060	0.61	0.047	0.024	35.0	0.021	0.90	3.99	0.084	0.027
2-2, 49	9.89	0.368	0.651	0.116	1.26	0.254	0.061	28.4	0.024	2.94	8.99	0.091	0.035
2-2, 129	10.69	0.244	0.679	0.124	1.47	0.295	0.071	26.6	0.025	3.57	10.62	0.104	0.044
2-3, 39	11.29	0.378	0.579	0.105	1.18	0.187	0.056	29.7	0.022	2.53	11.44	0.100	0.045
2-3, 129	12.29	0.214	0.451	0.089	0.86	0.080	0.043	33.0	0.021	1.55	5.58	0.092	0.027
2-4, 39	12.79	0.100	0.424	0.091	0.83	0.062	0.041	33.3	0.021	1.33	5.28	0.091	0.026
2-4, 139	13.79	0.129	0.433	0.094	0.89	0.059	0.043	33.4	0.021	1.42	5.66	0.091	0.027
2-5, 79	14.69	0.149	0.481	0.098	1.05	0.136	0.055	31.6	0.022	2.01	6.81	0.089	0.030
2-6, 79	16.19	0.233	0.550	0.106	1.30	0.217	0.063	29.0	0.024	2.77	8.52	0.092	0.035
2-6, 149	16.89	0.369	0.722	0.111	1.84	0.229	0.082	25.0	0.024	4.23	11.72	0.099	0.037
3-1, 9	16.99	0.069	0.489	0.070	1.27	0.174	0.047	29.4	0.022	2.67	8.55	0.094	0.041
3-1, 19	17.09	0.058	0.398	0.058	0.93	0.094	0.035	32.8	0.021	1.76	5.85	0.085	0.034
3-1, 29	17.19	0.085	0.416	0.062	0.99	0.089	0.036	32.6	0.021	1.73	6.28	0.085	0.036
3-1, 39	17.29	0.174	0.585	0.086	1.59	0.191	0.055	27.1	0.024	3.39	10.26	0.102	0.042
3-1, 49	17.39	0.343	0.685	0.099	1.88	0.269	0.060	24.6	0.026	4.16	12.31	0.097	0.032
3-1, 59	18.09	0.141	0.451	0.086	1.02	0.072	0.047	32.4	0.021	1.63	6.07	0.086	0.026
3-1, 89	18.39	0.181	0.571	0.084	1.68	0.337	0.067	27.2	0.026	3.57	9.86	0.103	0.052
3-1, 99	18.49	0.175	0.533	0.070	1.37	0.300	0.057	29.1	0.025	3.10	8.23	0.096	0.046
3-1, 109	18.59	0.208	0.668	0.080	1.84	0.273	0.066	25.3	0.024	3.75	11.52	0.103	0.049
3-1, 130	18.80	0.257	0.683	0.102	1.87	0.303	0.074	25.0	0.025	4.04	11.19	0.102	0.051
3-2, 19	19.29	0.186	0.536	0.070	1.24	0.369	0.047	29.7	0.024	2.92	7.72	0.087	0.044
3-2, 29	19.39	0.258	0.631	0.084	1.73	0.428	0.068	26.5	0.025	3.61	10.57	0.098	0.054
3-2, 49	19.59	0.311	0.656	0.117	1.82	0.321	0.080	27.0	0.025	3.64	9.93	0.101	0.044
3-2, 59	19.69	0.161	0.533	0.074	1.46	0.296	0.059	28.6	0.024	3.18	8.73	0.096	0.047
3-2, 87	19.97	0.213	0.747	0.088	2.08	0.223	0.075	23.3	0.024	4.52	13.01	0.106	0.048
3-2, 100	20.10	0.240	0.636	0.091	1.68	0.468	0.063	26.5	0.025	3.72	10.14	0.097	0.050
3-2, 129	20.39	0.285	0.714	0.093	1.86	0.284	0.068	24.6	0.026	4.19	11.89	0.100	0.047
3-2, 139	20.49	0.223	0.624	0.079	1.56	0.285	0.059	27.2	0.025	3.57	9.79	0.094	0.043
3-3, 9	20.59	0.369	0.640	0.117	1.59	0.332	0.073	27.3	0.027	3.37	9.25	0.091	0.035
3-3, 39	20.89	0.074	0.377	0.093	0.99	0.040	0.047	33.6	0.021	0.97	4.80	0.090	0.025
3-3, 109	21.69	0.152	0.460	0.092	1.32	0.073	0.047	30.9	0.023	1.95	7.68	0.106	0.035
3-3, 119	21.79	0.129	0.452	0.085	1.25	0.067	0.045	31.4	0.022	1.82	7.02	0.099	0.035
3-3, 139	21.99	0.159	0.516	0.099	1.43	0.078	0.049	30.3	0.022	2.24	8.30	0.111	0.035
3-3, 149	22.09	0.183	0.499	0.085	1.28	0.070	0.045	31.4	0.021	2.01	7.23	0.097	0.034
3-4, 19	22.29	0.038	0.304	0.059	0.79	0.039	0.030	34.7	0.021	0.91	3.96	0.091	0.030
3-4, 89	22.89	0.176	0.498	0.089	1.20	0.108	0.056	31.0	0.021	2.05	6.96	0.088	0.027
3-4, 129	23.19	0.080	0.475	0.066	1.27	0.188	0.051	29.6	0.021	2.60	7.96	0.097	0.040
3-5, 49	24.00	0.357	0.700	0.108	1.96	0.401	0.083	24.9	0.022	3.84	11.44	0.100	0.045
3-6, 69	25.69	0.561	0.733	0.113	2.03	0.344	0.084	24.4	0.023	4.00	11.82	0.096	0.040
3-6, 149	26.49	0.201	0.578	0.067	1.58	0.273	0.060	27.4	0.021	3.50	10.55	0.095	0.042
4-1, 79	27.89	0.362	0.704	0.130	1.89	0.349	0.081	24.9	0.025	3.90	11.46	0.095	0.035
4-2, 69	29.29	0.390	0.790	0.129	2.17	0.158	0.091	22.9	0.024	4.43	13.10	0.100	0.031
4-3, 19	30.29	0.009	0.401	0.062	0.99	0.065	0.038	31.6	0.021	1.77	6.87	0.092	0.035
4-3, 49	30.59	0.252	0.633	0.132	1.61	0.226	0.072	27.5	0.026	3.08	10.20	0.096	0.038
4-4, 80	32.40	0.359	0.729	0.113	1.82	0.287	0.081	24.8	0.024	3.92	11.67	0.097	0.039
4-4, 119	34.29	0.436	0.803	0.140	1.93	0.442	0.085	22.9	0.026	4.42	12.69	0.104	0.047
4-6, 49	35.09	0.667	0.827	0.166	1.93	0.318	0.085	23.0	0.030	4.37	12.78	0.098	0.040

icant difference in composition for Ca and Al between AA and XRF analysis. When analyzed by XRF, Si, Mn, and Fe were consistently higher, averaging 9.2%, 13.1%, and 8.4% higher, respectively, than Dymond's AA analyses. Barium by XRF averaged 6.5% lower than by AA. By comparing our results with other N.B.S. standard carbonate mixtures run separately from our calibration, we estimate that phosphorus may be 7.5% higher by our XRF analysis. I do not have reliable carbonate-rich standards at the proper elemental concentrations for Na, Mg, K, Ti, and S, but I assume that the accuracy of these elemental analyses is similar to that of the elements checked.

SEDIMENT COMPOSITION

$CaCO_3$

The major trends in $CaCO_3$ content of Leg 92 sediments (Fig. 3) are due to two major effects—dilution by hydrothermal sediments near the rise crest and dissolution of $CaCO_3$ as the Pacific Plate descends below the lysocline.

Carbonate contents are between 60 and 70% in the basal 20 m of each hole but rise to 90% higher in the section. The increase in carbonate above the basal section cannot be due to postdepositional dissolution, since there is little evidence for diagenesis except in the most basal 1 to 2 m of sediment. Dissolution due to lysocline effects does not explain why, in three different time periods (27 to 18 Ma or 51.3 to 20.9 m depth in Hole 597; 15.9 to 7 Ma or 43.2 to 7.0 m depth in Hole 598; and 8.1 Ma to the present or 35.1 to 0 m depth in Hole 599), carbonate contents increase as the water depth of each site increases. The best explanation for the common carbonate trend is dilution by significant quantities of hydrothermal sediments while the site is at the EPR crest; the dilution of carbonate decreases upcore as each site moves away from the ridge.

Holes 598 and 597, being on older, deeper oceanic crust, have penetrated the lysocline. In Hole 598 this zone is marked by highly variable but decreasing carbonate contents in the upper 6 m of the core, whereas in Hole 597 it is marked by a 2-m-thick sediment layer with low carbonate contents. The carbonate profiles of the Leg 92 sediments are discussed in more detail by Leinen (this volume).

Fe/Al

Previous work by Boström and Peterson (1969), Dymond et al. (1973), and others has shown that the basal metalliferous (hydrothermal) sediments at the EPR are highly enriched in Fe. This is true of the Leg 92 sediments as well. Figure 4 is a plot of the Fe/Al ratio (to eliminate dilution effects by $CaCO_3$) versus depth at the three holes. The figure shows that Sites 598 and 599 have Fe/Al values that decrease from very high (60 to 100) in the basal sediments to values between 3 and 10 at the present sediment surface. At Hole 597, however, Fe/Al changes cyclically from 9 to 30 over the depth range from 4 m to the basement (17 Ma to 28.3 Ma). From 4 m to the surface (17 Ma to the present), Fe/Al decreases mono-

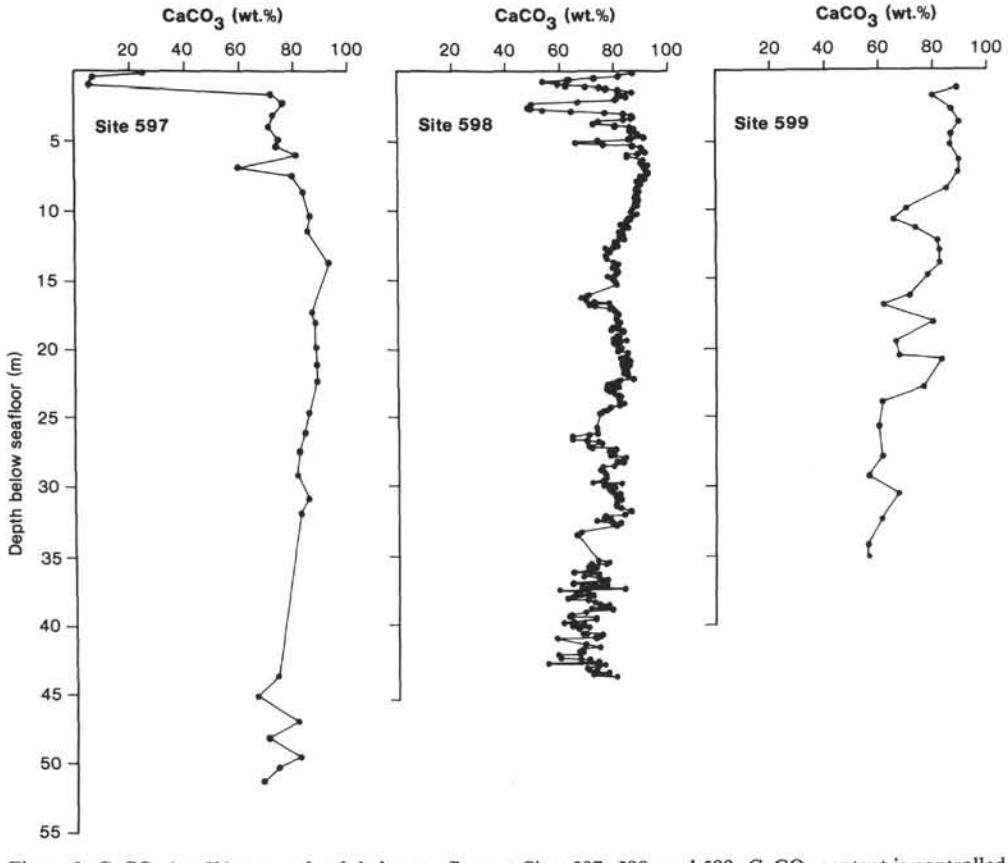

Figure 3. $CaCO_3$ (wt.%) versus depth below seafloor at Sites 597, 598, and 599. $CaCO_3$ content is controlled by dilution with hydrothermal precipitates in the basal sediments and by dissolution before burial in the core tops after each core passes through the lysocline.

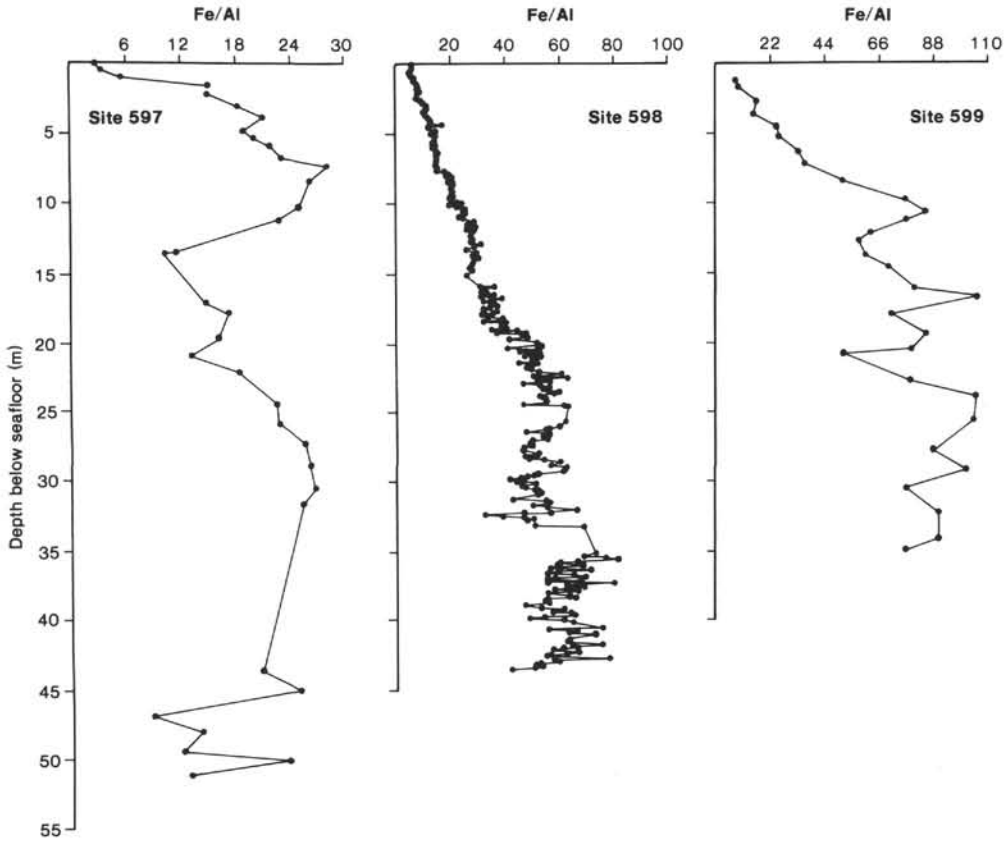

Figure 4. Fe/Al versus depth below seafloor at Sites 597, 598, and 599. Site 597 is marked by the lowest Fe/Al ratio and highest Al content.

tonically to a ratio near 3. The difference in average Fe/Al between the three sites is almost entirely due to higher Al contents at Holes 597 and 598. At all three sites, the average iron concentration for the basal 10 m of sediment is between 8 and 10%. The average aluminum content for the basal 10 m of Hole 597, however, is 0.47%, as compared with 0.15% at Hole 598 and 0.13% at Hole 599. The data suggest that Hole 597 had an additional source of aluminum as compared with the other two sites (perhaps some type of aluminosilicate detritus). The general decrease in Fe/Al upcore, as each site travels away from the source of hydrothermal sediments at the rise crest, is consistent with a general decrease of hydrothermal influence away from the ridge and an increase relative abundance of low-Fe/Al aluminosilicate debris.

Si/Al

Si/Al ratio at Sites 597, 598, and 599, like Fe/Al ratio, is high while the sites are at the rise crest and decreases as the sites move away (Fig. 5). Again, the major differences between the sites are due primarily to the average aluminum content of the sediments. The Si/Al ratios in the basal sediments of Holes 598 and 599 are similar to the hydrothermal Si/Al ratio of 11 found by Dymond (1981), and the Si/Al ratio of 3 at the top of all three cores is similar to the value estimated by Dymond for both authigenic and detrital end members. The Si/Al trends fit with mixing between hydrothermal precipitates and either authigenic material precipitating from seawater or aluminosilicate detritus.

Fe/P

Berner (1973) and Froelich et al. (1977) have suggested that iron oxyhydroxide precipitates, which are a large fraction of metalliferous sediments, can adsorb and remove significant amounts of phosphorus from the world ocean. Froelich et al. (1977) have estimated that about 15 to 40% of the total riverine flux of P is buried annually as the result of scavenging onto hydrothermal precipitates and their subsequent burial. Berner's (1973) study indicates that the amount of phosphorus contained in metalliferous sediments is primarily adsorbed and in equilibrium with dissolved phosphorus in seawater. If seawater phosphorus concentrations have not changed, it is not surprising that the basal sediments at all three sites have a mean Fe/P ratio between 60 and 80 (Fig. 6). There is an unexpectedly high degree of variability about the mean of this ratio, however, and an unexpected decrease in Fe/P occurs at the tops of Holes 597 and 598. A plot of phosphorus against iron (Fig. 7) suggests that the phosphorus contents of the sediments can be explained by the mixing of three end members: calcite (0% P, 0% Fe); a low-P, high-Fe end member; and a high-P, high-Fe end member. The low-P end member appears to be a typical hydrothermal precipitate. The high-P end member, because it is associated with the more slowly accu-

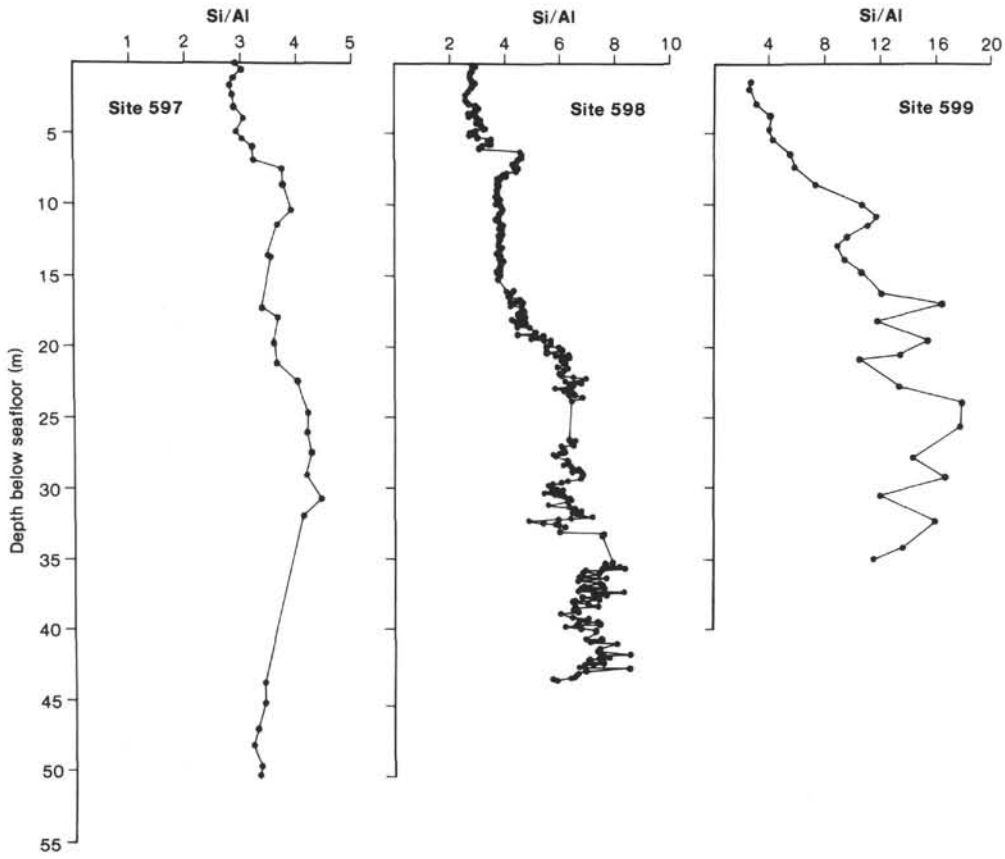

Figure 5. Si/Al versus depth below seafloor at Sites 597, 598, and 599.

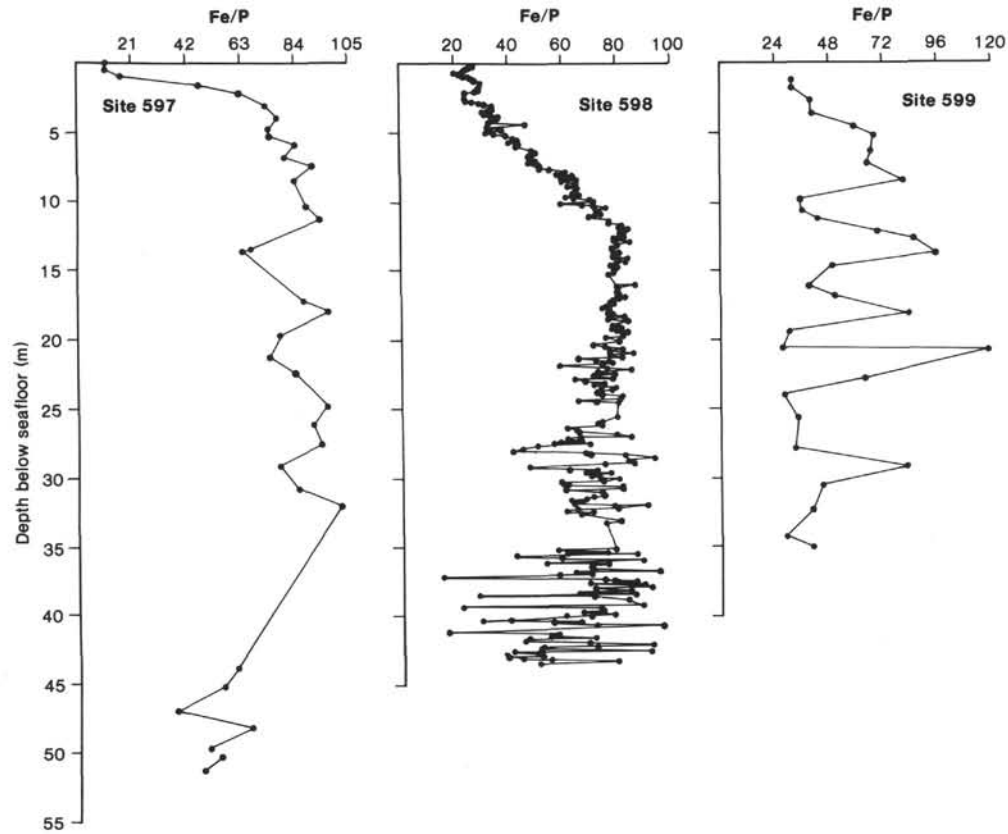

Figure 6. Fe/P versus depth below seafloor at Sites 597, 598, and 599.

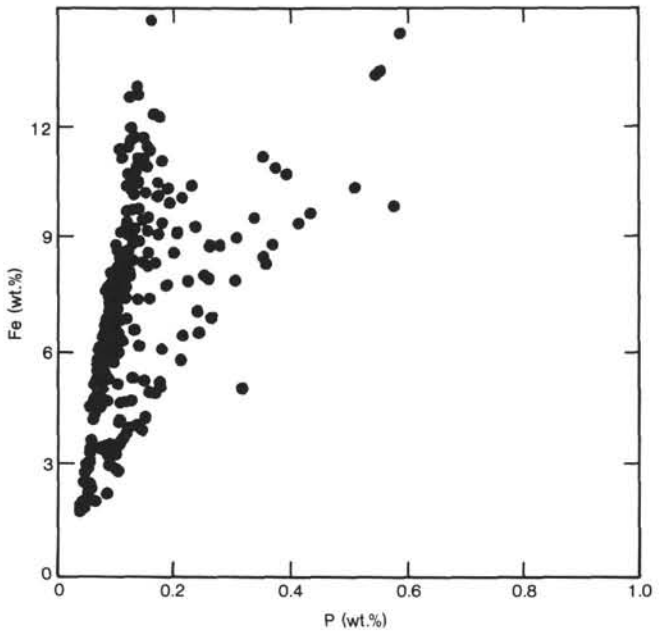

Figure 7. Fe (wt.%) plotted against P (wt.%) at Site 598. The distribution of data is consistent with mixing low Fe/P and high Fe/P end members with calcite.

mulating surface sediments, probably represents either additional phosphorus scavenged by the precipitates or the increase in the relative abundances of phosphatic fish debris in the slowly accumulating surface sediments. The variability of Fe/P in the basal sediments may indicate that hydrothermal activity is intermittent and separated by more slowly accumulating sediments or that the phosphorus content of Pacific Ocean waters has changed drastically on a relatively short time scale.

Fe/Mn

The Fe/Mn distribution in Leg 92 sediments was unexpected (Fig. 8). Dymond's (1981) study suggests that the basal sediments should have a "hydrothermal" ratio of about 3. Upcore, the Fe/Mn ratio should trend toward the authigenic end member ratio of 0.5, since there are low amounts of detrital material in the samples. The basal samples in all three cores have ratios of 3 but increase rather than decrease upcore. Only within the uppermost 2 to 4 m in each core (the sediments deposited farthest from the EPR) does the ratio of Fe to Mn begin to decrease. Even the surface sediments have Fe/Mn values greater than 3, however.

To attempt to explain this unexpected trend I generated four hypotheses:

1. Changes in the type of hydrothermal activity over time may have resulted in times when iron-rich hydrothermal precipitates were more common and the average Fe/Mn ratio of the sediments was higher.

2. The sediments more distal from the EPR may represent a mixture of Fe-rich precipitates derived from an off-ridge hydrothermal source and ridge-derived hydrothermal precipitates.

3. The change in Fe/Mn may mark the removal of manganese-rich particles from the hydrothermal plume, so that the deposits with high Fe/Mn ratios represent typical distal hydrothermal deposits (those far from the EPR).

4. Diagenesis may have reduced and remobilized manganese and left behind an iron-rich solid fraction.

Hypothesis 1 (that the hydrothermal effluent was richer in iron in the past) can be eliminated by comparing the Fe/Mn ratios that existed at the three sites over comparable periods of time. For example, between 5.4 and 8.6 Ma, or between 11.9 and 40.8 m depth, Site 599 was near the EPR crest and collected sediments with Fe/Mn values of about 3. During the same time period (between 4.7 and 10.9 m depth in Hole 598, and between 0.5 and 1 m depth in Hole 597), however, the Site 598 sediments have Fe/Mn ratios between 6 and 8, and the Site 597 sediments have ratios between 3.5 and 7. There is no period in time in which all three cores have Fe/Mn ratios that are consistently higher than in other time periods.

Data from surface sediments reported in Dymond (1981) and downcore data reported in this paper indicate a strong relationship between Fe/Mn and distance from the rise crest, not time. Figure 9 compares the Fe/Mn ratio to the distance from the rise crest at which the sediments were deposited for both sediments from the three Leg 92 holes and for surface sediments from the EPR. In each hole, depth in the sediment has been converted to distance from the rise crest by assuming a constant spreading rate and using the age–depth scales in Figure 2. The assumption of a constant spreading rate may introduce small errors, but they are not particularly important for this comparison. Figure 9 shows that the transition in Fe/Mn ratios in both modern and ancient sediments occurs on the ridge flanks, between 150 and 300 km from the rise axis. The high-Fe/Mn zones clearly do not mark time horizons but instead define a process related to distance from the rise crest.

Diagenetic remobilization of manganese (hypothesis 4) can be eliminated as a cause of high Fe/Mn ratio by both surface-sediment and downcore information. If diagenetic processes were removing manganese from the sediments, the surface sediments marked by high Fe/Mn more than 250 km from the EPR must now be losing extensive amounts of manganese to bottom waters. The pore water information obtained from this and other legs (Gieskes et al., this volume, for example) shows that nowhere in the area do sediments become sufficiently reducing for this to occur. In addition, the downcore Fe/Mn profiles require that times in the past were significantly more oxic to preserve the low Fe/Mn basal sediments. There is no evidence for a change in redox conditions here in the stable center of the South Pacific gyre.

The hydrothermal processes implicit in Hypothesis 2 (the off-ridge hydrothermal source hypothesis) are unlikely to occur. If Hypothesis 2 is true, an off-ridge hydrothermal system must be located at least 100 km from the crest of the EPR and must emit hydrothermal fluids rich in iron.

Experimental studies have outlined the restricted conditions that can produce hydrothermal fluids high in iron (Bischoff and Dickson, 1975; Seyfried and Bischoff, 1977, 1979; Mottl et al., 1979; Seyfried and Mottl, 1982). Ex-

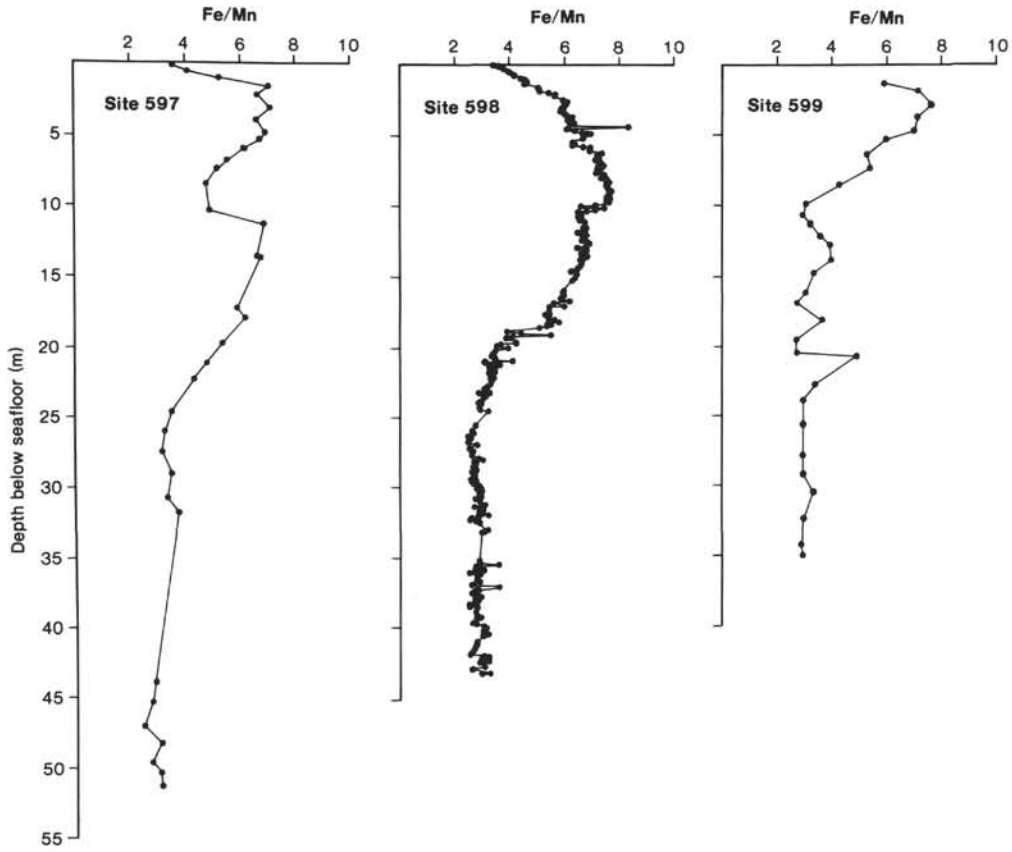

Figure 8. Fe/Mn profiles at Sites 597, 598, and 599. Low Fe/Mn ratio (≈ 3) in basal sediments is similar to that observed by Dymond (1981). High Fe/Mn near the core tops is not predicted by Dymond's model, however.

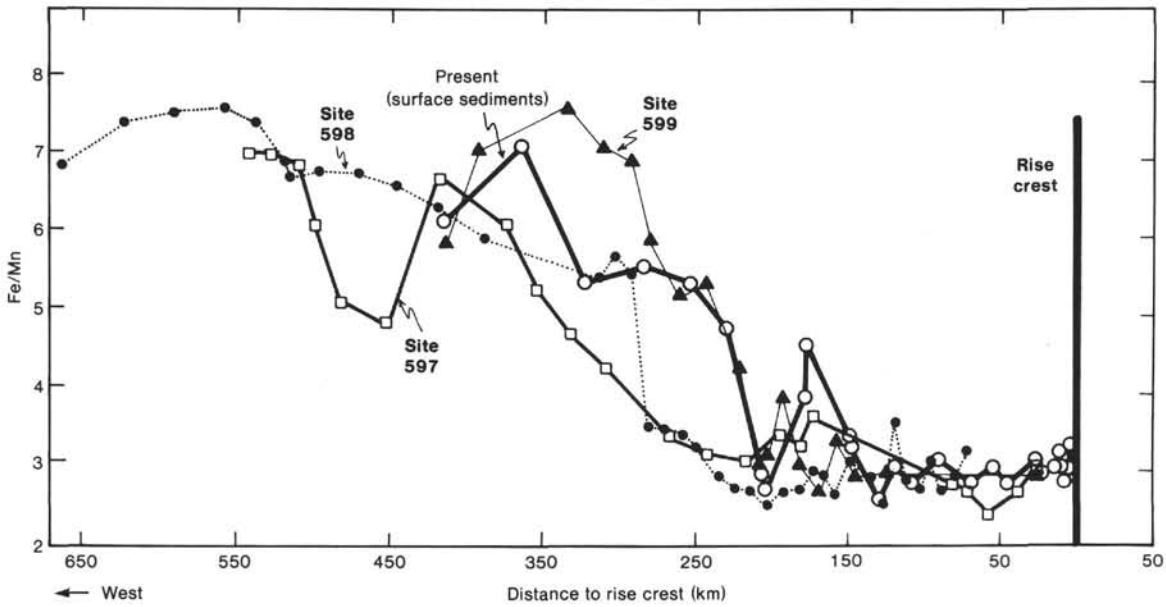

Figure 9. Comparison of Fe/Mn ratios in Leg 92 cores to Fe/Mn in modern sediments (open circles). The transition from low to high Fe/Mn occurs at approximately the same distance from the rise crest in ancient and modern sediments. The process that causes the change is still active today.

perimental fluids with Fe/Mn ratios greater than 5 have been produced only at temperatures greater than 400°C at low water/rock ratios (Mottl et al., 1979). At high water/rock ratios (>50; Seyfried and Mottl, 1982), the temperature at which high solution Fe/Mn occurs is only slightly lower (300°C).

Thus, if the high Fe/Mn ratio is due to additional hydrothermal activity, an extensive off-ridge hydrothermal source must exist at least 100 km from the spreading axis and must emit fluids as hot as the hottest hydrothermal fluids found at the spreading axis (RISE Project Group, 1980). Such high-temperature, off-ridge hydrothermal systems have been neither observed nor predicted (Anderson and Hobart, 1976; Lister, 1977).

The third hypothesis (that the deposits with high Fe/Mn ratios represent distal hydrothermal material) conflicts with speculations by Edmond et al. (1979) that hydrothermal Fe/Mn ratios in ferromanganese oxyhydroxide precipitates result from the saturation of surfaces of an initial Fe-rich oxyhydroxide precipitate with more slowly oxidizing manganese. By that model, the most distal hydrothermal deposits should either have a constant Fe/Mn ratio or be rich in manganese, because Mn is precipitated more slowly than Fe.

The compositional data from Leg 92 show that the most distal deposits are the richest in iron, however, and present an apparent paradox: the sediments deposited farthest from the EPR crest are most enriched in the element that should precipitate first from the hydrothermal fluid. The paradox can be resolved if one realizes that precipitation is not equivalent to sedimentation and burial. If a precipitate has a small enough particle size, it can drift for hundreds, perhaps thousands of kilometers before settling to the bottom.

The rapid mixing of hydrothermal fluids with normal seawater, as observed at 21°N, results in a large size range of iron-rich oxyhydroxide particulates and more coarse-grained sulfides. Even though most of this material will settle out rapidly, a small fraction of the precipitating material will be both colloidal in size and rich in iron. This was in fact first observed in the early studies of EPR sediments (Boström and Peterson, 1966). This fraction can drift far from the rise crest. Manganese, on the other hand, even though it should remain dissolved in seawater longer than iron, is essentially an insoluble element in oxygenated seawater and is readily scavenged onto falling particles (Weiss, 1977; Martin and Knauer, 1983). Dissolved manganese can therefore be stripped from the water column by falling particulates long before colloidal iron-rich oxyhydroxide particles will have settled to the bottom. Distal hydrothermal deposits more than 200 km from the rise crest can therefore be rich in iron even though iron is more rapidly precipitated than manganese.

FACTOR ANALYSIS OF LEG 92 SEDIMENTS

Factor analysis, as proposed by Miesch (1976) and by Leinen and Pisias (1984), provides a way to deduce the chemical composition of hypothetical end members in mixtures such as Leg 92 sediments and a way to see whether the chemical composition of distal deposits at the EPR are consistent with the hypothesis that an iron-rich fraction drifted from the rise crest. A factor analysis of the combined data set from Sites 597, 598, and 599 shows that three factors can explain 97% of the compositional variance in the data set (Table 2). The factors (end members) chosen by this more objective method reinforce the conclusions drawn in earlier sections.

Factor 1, which explains 43% of the total variance in the data set, is typical of hydrothermal material. It is dominated by Mn, Fe, and P (possibly because of coprecipitation with Fe, as suggested by Berner [1973]), and it dominates the sediment mixture at the base of each Leg 92 site. Factor 2, which explains 36% of the data variance, is dominated by Ca, K, and Ba and apparently represents biogenic calcite and barite. The Ba/S weight ratio in the end member is 3.6, similar to a stoichiometric barite (Ba/S = 4.3). The factor's distribution is similar to the calcite distribution in each core.

I call Factor 3, which explains 18% of the data variance, the distal factor. The distribution downcore of Factor 3 (Fig. 10) points out its distal association. It only dominates the sediment assemblage at the top of each core and is relatively low in importance downcore, where each site was near the rise crest. The factor is dominated by Al, Si, Ti, and P, all associated with slowly accumulating aluminosilicate debris or with apatitic fish debris. It is also marked by very high Fe contents. The Fe/Si ratio in the distal factor is 2.8, as compared with 1.2 in the most iron-rich hydrothermal clays (e.g., nontronite N1; Corliss et al., 1978). Clearly, excess iron oxyhydroxides are present in the factor. From these observations and from its dominance only in slowly accumulating sediments, the distal factor is probably a mixture of aluminosilicates, slowly accumulating apatitic fish debris, and very fine-grained iron-rich hydrothermal precipitates that have drifted far from the rise crest. The presence of aluminosilicates, shown by the high Al and Si loadings, probably represents fine-grained eolian detritus. I interpret the high P loading in this factor to be due to apatitic fish debris.

Table 2. Results of factor analysis of the combined Site 597, 598, and 599 data.[a]

	Factor 1 (hydrothermal)		Factor 2 (biogenic)		Factor 3 (distal)	
Element	Composition (wt.%)	Factor score[b]	Composition (wt.%)	Factor score[2]	Composition (wt.%)	Factor score[b]
Na	0.328	1.370	0	−0.309	0.779	0.505
Mg	0.840	0.975	0.268	0.582	1.74	0.048
Al	0	−0.584	0.078	0.285	3.39	2.577
Si	1.24	0.562	0.284	0.151	8.45	1.096
P	0.218	1.117	0	−0.524	0.990	1.109
K	0.971	0.404	1.08	1.594	1.49	−0.350
Ca	21.6	0.197	40.2	2.130	0	−0.682
Ti	0.013	−0.132	0.022	0.837	0.293	1.302
Mn	5.18	2.215	0	−0.506	2.27	−0.448
Fe	13.2	1.365	1.59	0.095	23.7	0.095
Ba	0.055	0.090	0.090	1.579	0.300	0.105
S	0.045	0.519	0.025	0.805	0.199	0.408
Variance[c]	43%		36%		18%	

[a] The data were weighted by normalization to equal means; resulting factors were rotated by the VARIMAX algorithm and compositions determined by the QROTATE algorithm of Leinen and Pisias (1984).

[b] Factor score is a measure of the importance of each element in determining the factor. High factor scores mark elements dominating the factor.

[c] Variance given is the percent of the total sums of squares in the data set explained by the factor.

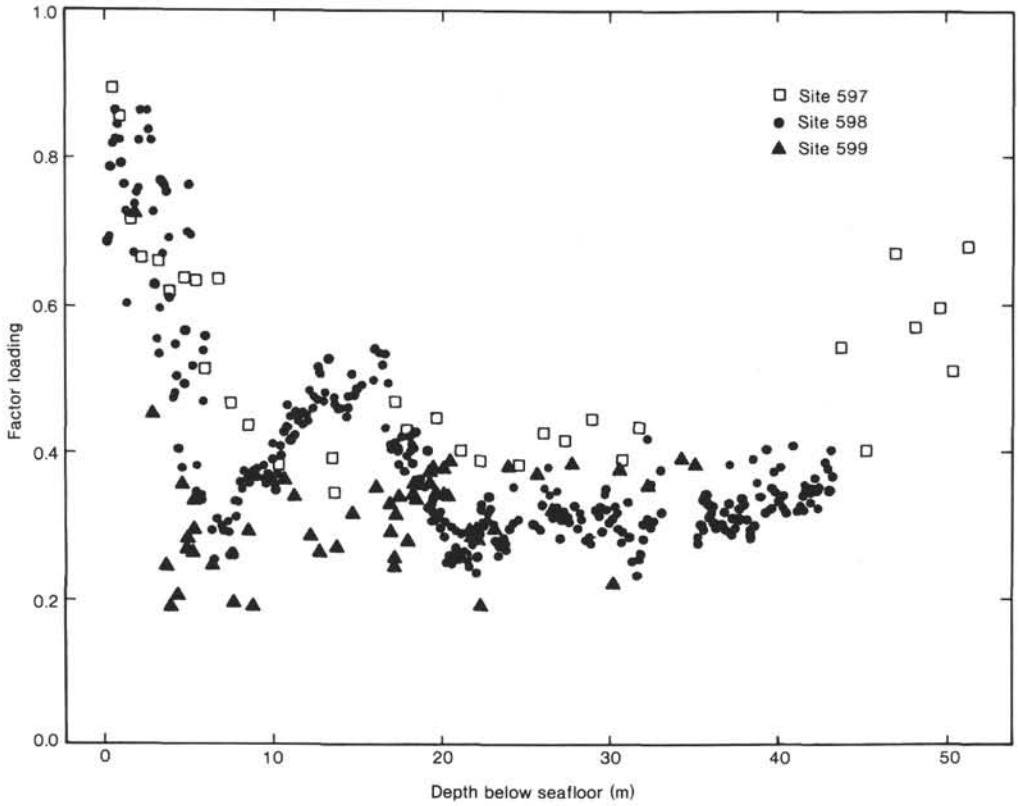

Figure 10. Depth distribution of the distal factor (see Table 2 and text) at Sites 597, 598, and 599. The distal factor only dominates in the slowly accumulating sediments in the top of each core.

CONCLUSIONS

Leg 92 basal sediments contain hydrothermal precipitates similar to those described by Dymond (1981). There is no evidence for variations in basal sediment composition due to changes in the composition of hydrothermal source waters. Upcore there is strong evidence that precipitates carried in the hydrothermal plume become fractionated due to size-settling effects. Because of precipitation kinetics, iron-rich oxyhydroxides are precipitated first from the hydrothermal waters. Relatively coarse-grained material (probably >10 to 20 μm) settles out near the vents. It is eventually joined by the more slowly oxidizing hydrothermal manganese, which is stripped from the water column by both hydrothermal and biogenic particulate debris. The very fine-grained iron-rich particles drift far from the hydrothermal vents, eventually enriching distal deposits in Fe oxyhydroxides. Distal deposits west of the EPR, because they accumulate below the lysocline and are isolated from sediment source terrains, are sediments typical of central gyre regions. They also collect eolian aluminosilicates and apatitic fish debris, and they are unusual only in their high iron contents inherited from distant hydrothermal activity.

REFERENCES

Anderson, R. N., and Hobart, M. A., 1976. The relation between heat flow, sediment thickness, and age in the eastern Pacific. *J. Geophys. Res.*, 81:2968–2989.

Berner, R. A., 1973. Phosphate removal from sea water by adsorption on volcanogenic ferric oxides. *Earth Planet. Sci. Lett.*, 18:77–86.

Bischoff, J. L., and Dickson, F. W., 1975. Seawater–basalt interaction at 200°C and 500 bars: implications for origin of sea-floor heavy-metal deposits and regulation of seawater chemistry. *Earth Planet. Sci. Lett.*, 25:385–397.

Boström, K., and Peterson, M. N. A., 1966. Precipitates from hydrothermal exhalations on the East Pacific Rise. *Econ. Geol.*, 61: 1258–1265.

_____, 1969. The origin of aluminum-poor ferromanganoan sediments in areas of high heat flow on the East Pacific Rise. *Mar. Geol.*, 7:427–447.

Corliss, J. B., Lyle, M., Dymond, J., and Crane, C., 1978. The chemistry of hydrothermal mounds near the Galapagos Rift. *Earth Planet. Sci. Lett.*, 40:12–24.

Dymond, J., 1981. Geochemistry of Nazca Plate surface sediments: an evaluation of hydrothermal, biogenic, detrital, and hydrogenous sources. *In* Kulm, L. D., Dymond, J., Dasch, E. J., Hussong, D. M., and Roderick, R. (Eds.), *Nazca Plate: Crustal Formation and Andean Convergence.* Geol. Soc. Am. Mem., 154: 133–174.

Dymond, J., Corliss, J. B., Heath, G. R., Field, C. W., Dasch, E. J., and Veeh, H. H., 1973. Origin of metalliferous sediments from the Pacific Ocean. *Geol. Soc. Am. Bull.*, 84:3355–3372.

Dymond, J., Corliss, J. B., and Stillinger, R., 1976. Chemical composition and metal accumulation rates of metalliferous sediments from Sites 319, 320, and 321. *In* Yeats, R. S., Hart, S. R., et al., *Init. Repts. DSDP*, 34: Washington (U.S. Govt. Printing Office), 575–588.

Edmond, J. M., Measures, C., Mangum, B., Grant, B., Sclater, F. R., Collier, R., Hudson, A., Gordon, L. I., and Corliss, J. B., 1979. On the formation of metal-rich deposits at ridge crests. *Earth Planet. Sci. Lett.*, 46:19–30.

Froelich, P. N., Bender, M. L., and Heath, G. R., 1977. Phosphorus accumulation rates in metalliferous sediments on the East Pacific Rise. *Earth Planet. Sci. Lett.*, 34:351–359.

Leinen, M., and Pisias, N., 1984. An objective technique for determining end-member compositions and for partitioning sediments according to their sources. *Geochim. Cosmochim. Acta*, 48:47–62.

Lister, C. R. B., 1977. Qualitative models of spreading-center processes, including hydrothermal penetration. *Tectonophysics*, 37:203–218.

Lupton, J. E., and Craig, H., 1981. A major helium-3 source at 15°S on the East Pacific Rise. *Science*, 214:13–18.

Martin, J. H., and Knauer, G. A., 1983. VERTEX: manganese transport with $CaCO_3$. *Deep-Sea Res.*, 30:411–425.

Miesch, A. T., 1976. Q-mode factor analysis of geochemical and petrologic data matrices with constant row-sums. *Geol. Surv. Prof. Pap. U.S.*, 574-G:G1–G47.

Mottl, M. J., Holland, H. D., and Corr, R. F., 1979. Chemical exchange during hydrothermal alteration of basalt by seawater—II. Experimental results for Fe, Mn, and sulfur species. *Geochim. Cosmochim. Acta*, 43:869–884.

Reid, J. L., 1982. Evidence of an effect of heat flux from the East Pacific Rise upon the characteristics of the mid-depth waters. *Geophys. Res. Lett.*, 9:381–384.

RISE Project Group, 1980. East Pacific Rise: hot springs and geophysical experiments. *Science*, 207:1421–1433.

Seyfried, W., and Bischoff, J. L., 1977. Hydrothermal transport of heavy metals by seawater: the role of seawater/basalt ratio. *Earth Planet. Sci. Lett.*, 34:71–77.

_____, 1979. Low temperature basalt alteration by seawater: an experimental study at 70°C and 150°C. *Geochim. Cosmochim. Acta*, 43:1937–1947.

Seyfried, W. E., Jr., and Mottl, M. J., 1982. Hydrothermal alteration of basalt by seawater under seawater-dominated conditions. *Geochim. Cosmochim. Acta*, 46:985–1002.

Weiss, R. F., 1977. Hydrothermal manganese in the deep sea: scavenging residence time and Mn/3-He relationships. *Earth Planet. Sci. Lett.*, 37:257–262.

Yeats, R. S., Hart, S. R., et al., 1976. *Init. Repts. DSDP*, 16: Washington (U.S. Govt. Printing Office).

Date of Initial Receipt: 13 July 1984
Date of Acceptance: 5 February 1985